Molecular Therapy
Nucleic Acids
Original Article

Kcnq1ot1/miR-381-3p/ETS2 Axis Regulates Inflammation in Mouse Models of Acute Respiratory Distress Syndrome

Xiaohui Jiang,[1,2,5] Meihong Yu,[1,5] Taiping Zhu,[1] Lulu Lou,[3] Xu Chen,[2] Qian Li,[2] Danhong Wei,[4] and Renhua Sun[2]

[1]Department of Critical Care Medicine, Chun'an First People's Hospital (Zhejiang Provincial People's Hospital, Chun'an Branch), Hangzhou 311700, P.R. China; [2]Department of Critical Care Medicine, Zhejiang Provincial People's Hospital, People's Hospital of Hangzhou Medical College, Hangzhou 310014, P.R. China; [3]Internal Medicine, Zhejiang Chinese Medical University, Hangzhou 310053, P.R. China; [4]Department of Neuroscience Care Unit, The Second Affiliated Hospital, College of Medicine, Zhejiang University, Hangzhou 310009, P.R. China

Inflammatory mediators play a key role in the pathogenesis of acute respiratory distress syndrome (ARDS). In this study, we aimed to explore the involvement of the Kcnq1 opposite strand/antisense transcript 1 (Kcnq1ot1)/miR-381-3p/E26 transformation-specific proto-oncogene 2 (ETS2) axis in inflammation of lipopolysaccharide (LPS)-induced ARDS. Microarray analysis revealed ETS2 as an upregulated gene in ARDS. Then, a LPS-induced ARDS mouse model was constructed, with a series of gain- or loss-of-function experiments conducted to evaluate the lung function and neutrophil extracellular trap (NET) formation in lung tissue and determine the neutrophil number, myeloperoxidase (MPO) activity, and inflammatory factor levels in bronchoalveolar lavage fluid (BALF). As the results revealed, downregulated expression of ETS2 resulted in improved lung function, decreased NETs, MPO activity, and levels of interleukin (IL)-6 and tumor necrosis factor alpha (TNF-α), as well as increased IL-10 level. Then, the assays of dual-luciferase reporter, RNA-binding protein immunoprecipitation (RIP), and RNA pull-down were performed to validate that Kcnq1ot1 promoted ETS2 expression by competitively binding to miR-381-3p. Meanwhile, it was also found that Kcnq1ot1 silencing reversed the promotive effect of EST2 on ARDS. Our results provide evidence that Kcnq1ot1 silencing may reduce the inflammatory response in LPS-induced ARDS via inhibition of miR-381-30-dependent ETS2, thereby presenting new molecular understanding for the development of ARDS.

INTRODUCTION

Acute respiratory distress syndrome (ARDS) is a major clinical presentation of acute lung injury, characterized by decreased lung compliance, noncardiogenic pulmonary edema, and refractory hypoxia.[1] Severe ARDS remains deadly, with a mortality rate of approximately 40%, despite advancements in supportive care.[2] ARDS develops as an inflammatory process in response to extrapulmonary and pulmonary stimuli to the alveolar-capillary membrane, leading to increased vascular permeability and subsequently pulmonary edema.[3] Pulmonary neutrophilic inflammation is a principal process triggering ARDS during microbial infection in the alveolar microenvironment.[4,5] Furthermore, elevation of neutrophil recruitment, myeloperoxidase (MPO) activity, and reactive oxygen species (ROS) found in lungs from ARDS mice favors the formation of neutrophil extracellular traps (NETs).[6] NETs, representing a danger-associated molecular pattern, associate with inflammatory reactions and tissue injury in the lung.[7] Therefore, targeting NETs or a danger-associated molecular pattern may be a novel therapeutic direction for the treatment of ARDS.[7]

E26 transformation-specific proto-oncogene 2 (ETS2), a transcription factor in the ETS family, is a direct effector in the regulation of macrophage functions during inflammatory responses.[8] As a critical substrate of the mitogen-activated protein kinase (MAPK)/extracellular signal-regulated kinase (ERK) pathway, ETS2 modulates multiple genes induced by MAPK activation during tumor development.[9,10] ETS2 is a target of miR-381-3p, and the MAPK/miR-381 axis is involved in epithelial-mesenchymal transition in lung cancer.[11] More importantly, miR-381 is involved in the treatment of lipopolysaccharide (LPS)-induced acute lung injury by dexmedetomidine.[12] The same study also predicted that miR-381-3p was regulated by long non-coding RNA (lncRNA) Kcnq1 opposite strand/antisense transcript 1 (Kcnq1ot1) through competitive binding. Kcnq1ot1, located at human chromosome 11p15.5,[13] is a 91-kb-long RNA polymerase II-encoded nuclear transcript.[14] The stability of Kcnq1ot1 is critical for bidirectional gene silencing.[14] lncRNA Kcnq1ot1 is expressed at a high level in lung adenocarcinoma and acts as an oncogene to promote malignancy and chemoresistance in cancer cells.[15] Despite previous studies showing the involvement of miR-381-3p and Kcnq1ot1 in various lung diseases, their impact in ARDS is

Received 29 April 2019; accepted 28 October 2019;
https://doi.org/10.1016/j.omtn.2019.10.036.

[5]These authors contributed equally to this work.

Correspondence: Xiaohui Jiang, Department of Critical Care Medicine, Chun'an First People's Hospital (Zhejiang Provincial People's Hospital, Chun'an Branch), No. 1869, Huanhu North Road, Qiandaohu Town, Hangzhou 311700, Zhejiang Province, P.R. China.
E-mail: h_x2012@yeah.net

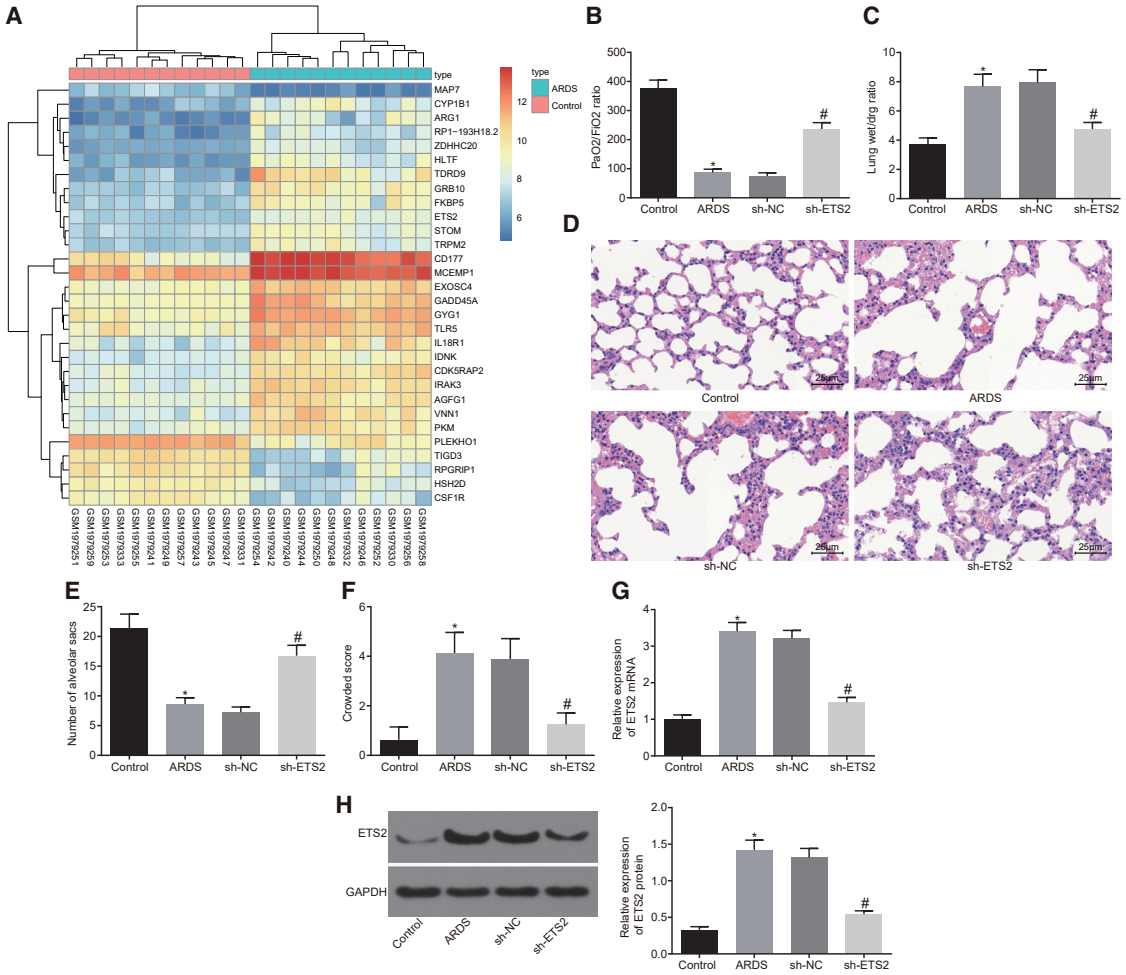

Figure 1. ETS2 Is Involved in LPS-Induced ARDS

(A) Heatmap of differential gene expression for ARDS-related expression dataset GSE76293. Abscissa indicates sample number, ordinate indicates differentially expressed gene, right upper histogram indicates color scale, and each rectangle in the panel corresponds to expression value in one sample. (B) Ratio of PaO_2/FiO_2. (C) Lung wet weight to dry weight ratio. (D) Pathological changes of lung parenchyma observed by H&E staining 48 h after induction of ARDS (original magnification, ×400). (E) Number of alveolar sacs determined after induction of ARDS. (F) Lung parenchymal score determined after induction of ARDS. (G) mRNA expression of ETS2 in peripheral blood of mice examined by qRT-PCR. (H) Protein levels and bands of ETS2 in peripheral blood of mice examined by western blot analysis. *$p < 0.05$ versus the control group; #$p < 0.05$ versus the sh-NC group. The measurement data are presented as mean ± SD. Comparison between two groups was analyzed by an unpaired t test, Welch's correction t test, and a Mann-Whitney test. n = 8.

currently unknown. Therefore, we aimed to investigate the role of the Kcnq1ot1/miR-381-3p/ETS2 axis in neutrophilic inflammation during ARDS.

RESULTS

ETS2 Is Involved in LPS-Induced ARDS

We first performed a differential gene expression analysis on an ARDS-related expression dataset, GSE76293. A heatmap illustrating the most differentially expressed genes is shown in Figure 1A and Table S1. Among all of the obtained differentially expressed genes, we noticed that the p value of the ETS2 gene was the smallest, and it was significantly highly expressed in ARDS. Therefore, the significantly upregulated ETS2 gene was identified as the target gene following differential analysis of the microarray. To explore the role of ETS2 in ARDS, we developed a mouse model. The ARDS mouse models induced by LPS for 48 h had a decreased ratio of the partial pressure of arterial oxygen (PaO_2)/percentage of inspired oxygen (FiO_2) (Figure 1B), increased lung wet weight to dry weight ratio (Figure 1C), reduced number of alveolar sacs (Figures 1D and 1E), and increased crowded score (Figure 1F) when compared to saline-treated controls. These results demonstrated the successful establishment of the ARDS mouse model.

The expression of ETS2 in peripheral blood was then detected by qRT-PCR and western blot analysis. Expression of ETS2 mRNA and protein was significantly increased in ARDS mice versus control

mice (Figures 1G and 1H, $p < 0.05$), thereby validating our bioinformatic findings. To study the effects of genetic manipulation of ETS2, we then silenced ETS2 in ARDS mice by treatment with short hairpin RNA (shRNA), which predictably resulted in a reduced expression of ETS2 in peripheral blood when compared with those treated with sh-negative control (NC) (Figures 1G and 1H, $p < 0.05$). Encouragingly, however, sh-ETS2 treatment also increased the ratio of PaO_2/FiO_2 (Figure 1B, $p < 0.05$) and decreased the lung wet weight to dry weight ratio when compared to sh-NC (Figure 1C, $p < 0.05$). A significantly increased number of alveolar sacs, as well as a significantly decreased crowded score, was observed in ARDS mice treated with sh-ETS2 versus sh-NC treatment (Figures 1D–1F, $p < 0.05$). Taken together, these results indicate that ETS2 is involved in the pathogenesis of LPS-induced ARDS.

Downregulated ETS2 Reduces Neutrophilic Inflammation in Lungs of ARDS Mouse Models

Having identified an involvement of ETS2 in ARDS mouse models, we continued to explore its effects on neutrophilic inflammation in the lung. The total cells and neutrophils were significantly recruited in the bronchoalveolar lavage fluid (BALF) of the ARDS mouse models, which were reduced in response to the sh-ETS2 treatment (Figure 2A, $p < 0.05$). At the same time, we found that the MPO activity and the levels of tumor necrosis factor alpha (TNF-α) and interleukin (IL)-6 in the BALF of the ARDS mouse models were significantly increased, accompanied by decreased IL-10, and these changes were reversed in the presence of sh-ETS2 treatment (Figures 2B and 2C, $p < 0.05$). MPO and histone are known biomarkers of NETs to identify neutrophilic inflammation. Indeed, when we performed an immunofluorescence assay, we found significantly increased NETs in the lung tissue of ARDS mouse models, and we showed that they could be diminished by treatment with sh-ETS2 (Figure 2D).

miR-381-3p Directly Targets the 3′ UTR of ETS2 mRNA

To identify putative microRNAs (miRNAs) binding to ETS2, we employed the prediction tools TargetScan (http://www.targetscan.org/vert_71/) and DIANA Tools (http://diana.imis.athena-innovation.gr/DianaTools/index.php?r=microT_CDS/index). Intriguingly, the candidate hit miR-381-3p was identified from both analysis pipelines (Figure 3A; Table S2). In an effort to validate our *in silico* finding, we assessed the expression of miR-381-3p in relationship to ETS2 and found that in neutrophils from BALF in ARDS mice, miR-381-3p expression was downregulated while that of ETS2 was upregulated (Figure 3B, $p < 0.05$). We then predicted potential binding sites of miR-381-3p to ETS2 by TargetScan (Figure 3C) and performed a dual-luciferase reporter assay to verify this prediction. Luciferase activity was significantly decreased when miR-381-3p agomir was co-transfected with ETS2 3′ UTR-wild-type (WT) when compared to co-transfection with agomir-NC and ETS2 3′ UTR-WT (Figure 3D). Luciferase activity was similar between co-transfection of miR-381-3p agomir with ETS2 3′ UTR-mutant (MUT) and co-transfection with agomir-NC and ETS2 3′ UTR-WT (Figure 3D). Moreover, expression of ETS2 mRNA and protein was significantly reduced after miR-381-3p agomir treatment in neutrophils from BALF in ARDS mice (Figures 3E and 3F, $p < 0.05$). Collectively, these results indicate that miR-381-3p targets and negatively regulates ETS2.

Kcnq1ot1 Competitively Binds to miR-381-3p to Promote ETS2 Expression

Through the DIANA Tools dataset, we further found that miR-381-3p had binding sites for Kcnq1ot1 (Figure 4A). Luciferase activity was significantly reduced when miR-381-3p was co-transfected with Kcnq1ot1-WT versus agomir-NC (Figure 4B, $p < 0.05$). We also observed that mRNA expression of Kcnq1ot1 in BALF neutrophils from ARDS mice was significantly increased when compared to control mice (Figure 4C, $p < 0.05$). RNA-binding protein immunoprecipitation (RIP) (Figure 4D) and RNA pull-down (Figure 4E) assays confirmed that Kcnq1ot1 indeed bound to miR-381-3p. We then designed two Kcnq1ot1 shRNAs to knock down Kcnq1ot1 in BALF neutrophils from ARDS mice. Silencing of Kcnq1ot1 in neutrophils resulted in a significant increase in mRNA expression of miR-381-3p, and a significant decrease in the expression of Kcnq1ot1 and ETS2, when compared to sh-NC (Figure 4F, $p < 0.05$). Taken together, these results confirm that Kcnq1ot1 competitively binds to miR-381-3p to promote ETS2 expression.

Kcnq1ot1/miR-381-3p/ETS2 Axis Regulates Inflammatory Response in ARDS Mouse Models

Having identified that Kcnq1ot1 regulates ETS2 expression through miR-381-3p, we focused our attention on further analyzing the role of the Kcnq1ot1/miR-381-3p/ETS2 axis in the inflammatory response in ARDS. Lung function tests revealed that the ratio of PaO_2/FiO_2 increased while the lung wet weight to dry weight ratio decreased in response to treatment of sh-Kcnq1ot1 + antagomir-NC, versus treatment with sh-NC + antagomir-NC. However, the ratio of PaO_2/FiO_2 and the lung wet weight to dry weight ratio induced by sh-Kcnq1ot1 + antagomir-NC were significantly decreased and increased, respectively, by treatment with the sh-Kcnq1ot1 + miR-381-3p antagomir. The ratio of PaO_2/FiO_2 was decreased while the lung wet weight to dry weight ratio was increased in response to sh-Kcnq1ot1 + ETS2, in comparison to treatment with sh-Kcnq1ot1 + vector-NC (Figures 5A and 5B, $p < 0.05$).

H&E staining of lung sections showed that the number of alveolar sacs was significantly increased, accompanied by lower lung parenchyma score in the presence of sh-Kcnq1ot1 + antagomir-NC, when compared to sh-NC + antagomir-NC. In addition, relative to sh-Kcnq1ot1 + antagomir-NC, treatment with sh-Kcnq1ot1 + miR-381-3p antagomir resulted in a decreased number of alveolar sacs and an increased lung parenchyma score. We also observed a reduced number of alveolar sacs and elevated lung parenchymal score in response to sh-Kcnq1ot1 + ETS2, versus sh-Kcnq1ot1 + vector-NC (Figures 5C–5E, $p < 0.05$).

Next, we measured the number of neutrophils and found that total cells and neutrophils in the BALF treated with sh-Kcnq1ot1 + antagomir-NC

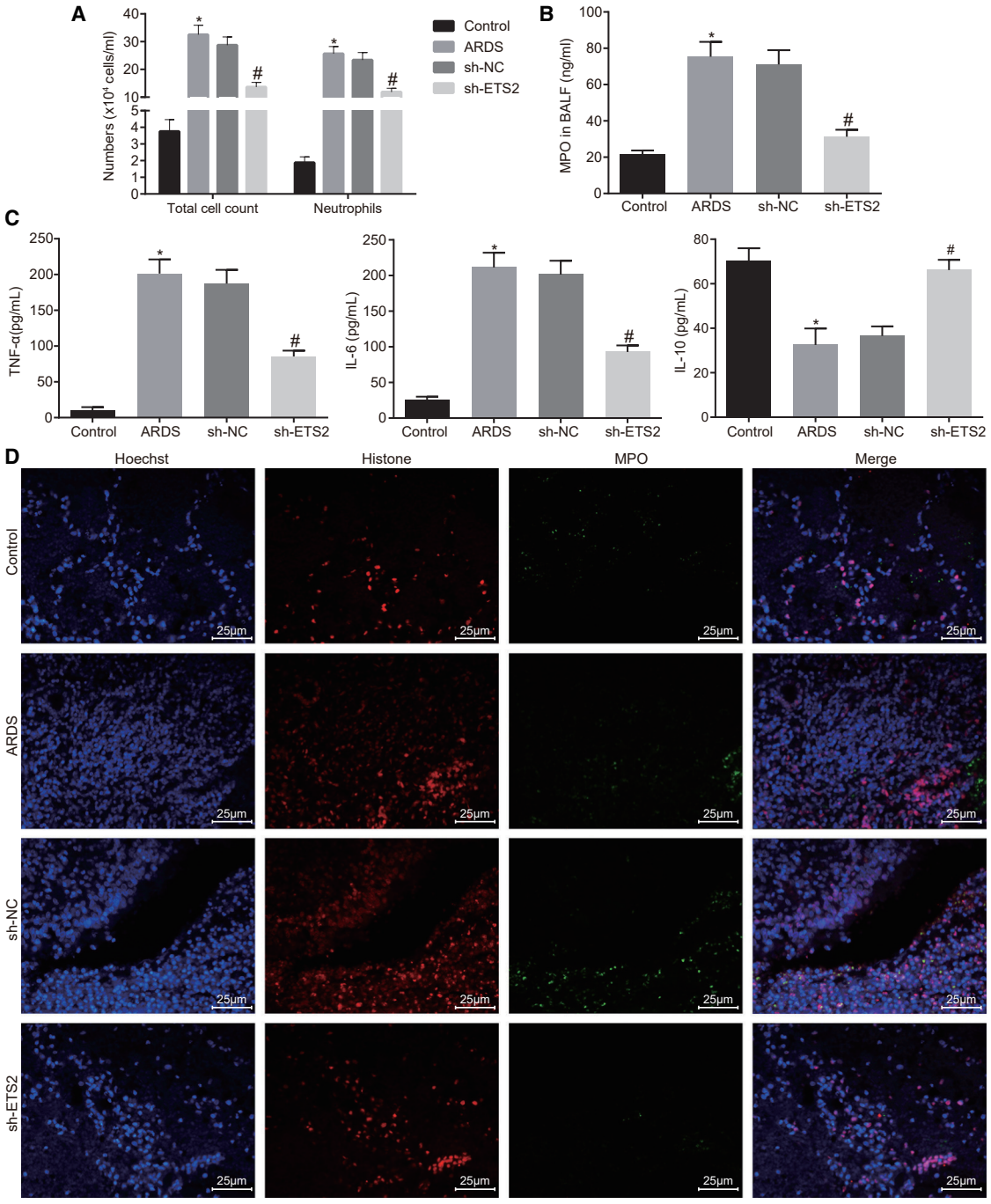

Figure 2. Silencing of ETS2 Attenuates Neutrophilic Inflammation in Lungs of ARDS Mouse Models

(A) Quantification of total cells and neutrophils in BALF of mice. (B) Quantification of MPO activity in BALF of mice. (C) Quantification of levels of TNF-α, IL-6, and IL-10 in BALF of mice as examined by ELISA. (D) Immunofluorescence detection of NETs formation (original magnification, ×400). *$p < 0.05$ versus the control group; #$p < 0.05$ versus the sh-NC group. The measurement data are presented as mean ± SD. Comparison between two groups was analyzed by an unpaired t test. n = 8.

were decreased compared to those treated with sh-NC + antagomir-NC. However, in contrast to treatment with sh-Kcnq1ot1 + antagomir-NC, the total cells and neutrophils in BALF with sh-Kcnq1ot1 + miR-381-3p antagomir treatment were increased. When compared with sh-Kcnq1ot1 + vector-NC treatment, both the total cells and neutrophils in BALF with sh-Kcnq1ot1 + ETS2 treatment were significantly

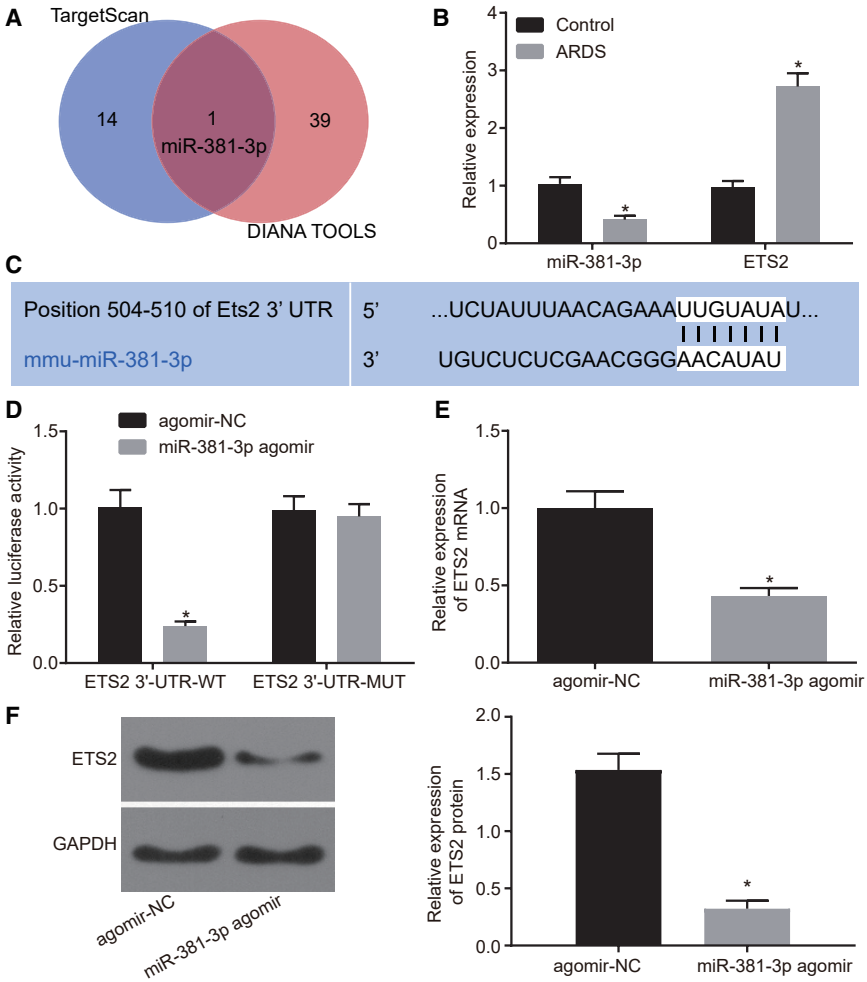

Figure 3. miR-381-3p Directly Targets the 3′ UTR of ETS2 mRNA

(A) miRNAs binding to ETS2 predicted by Targetscan and DIANA TOOLS. (B) Expression of miR-381-3p and ETS2 in BALF neutrophils in ARDS mouse models and mice in the control group examined by qRT-PCR (*$p < 0.05$ versus the control group). (C) Binding sites of miR-381-3p to ETS2 predicted by Targetscan. (D) Binding of miR-381-3p and ETS2 verified by the dual-luciferase reporter assay (*$p < 0.05$ versus the agomir-NC group). (E) Expression of ETS2 in BALF neutrophils of ARDS mouse models examined by qRT-PCR (*$p < 0.05$ versus the agomir-NC group). (F) Expression of ETS2 in neutrophils of BALF from ARDS mouse models examined by western blot analysis (*$p < 0.05$ versus the agomir-NC group). The measurement data are presented as mean ± SD. Comparison between two groups was analyzed by an unpaired t test. n = 8. The cell experiments were repeated three times.

enriched (Figure 5F, $p < 0.05$). At the same time, we found that compared with sh-NC + antagomir-NC treatment, the MPO activity in BALF treated by sh-Kcnq1ot1 + antagomir-NC was decreased, and the levels of TNF-α and IL-6 were decreased, accompanied by increased IL-10. Similarly, relative to the sh-Kcnq1ot1 + antagomir-NC treatment group, the BALF treated with sh-Kcnq1ot1 + miR-381-3p antagomir showed increased MPO activity and levels of TNF-α and IL-6, and a decreased level of IL-10. Additionally, in contrast to sh-Kcnq1ot1 + vector-NC treatment, the MPO activity and levels of TNF-α and IL-6 were increased, accompanied by decreased IL-10, in the BALF treated with sh-Kcnq1ot1 + ETS2 (Figures 5G and 5H, $p < 0.05$). Furthermore, as the immunofluorescence assay showed, compared to treatment with sh-NC + antagomir-NC, the presence of sh-Kcnq1ot1 + antagomir-NC resulted in reduced NETs in lung tissue of mice, and treatment with sh-Kcnq1ot1 + miR-381-3p antagomir displayed more NETs in lung tissue than did treatment with sh-Kcnq1ot1 + antagomir-NC. The sh-Kcnq1ot1 + ETS2 treatment group showed more NETs in the lung tissue than did the group treated with sh-Kcnq1ot1 + vector-NC (Figure 5I). Taken together, the aforementioned results suggest that the Kcnq1ot1/miR-381-3p/ETS2 axis could regulate the inflammatory response in ARDS mouse models.

DISCUSSION

ARDS is a high-incidence and sometimes life-threatening syndrome, and early diagnosis and treatment are therefore important for better outcomes.[16] Excessive neutrophilic inflammation has been shown to have a critical role in various lung conditions,[17,18] but its mechanism is largely unknown in the context of ARDS. lncRNA Kcnq1ot1 is involved in modulating imprinted genes in the Kcnq1 domain and facilitates the progression of non-small cell lung cancer through the miR-27b-3p/HSP90AA1 axis as an oncogene.[19] In this study, we uncover an important novel finding that the Kcnq1ot1/miR-381-3p/ETS2 axis regulates the inflammatory response in LPS-induced ARDS mice (a schematic diagram is shown in Figure 6).

We first identified ETS2 as the most significantly upregulated gene in ARDS according to microarray analysis of the ARDS-related GSE76293 expression dataset, and we validated that ETS2 indeed participated in the progression of LPS-induced ARDS. This result agrees with previous studies that ETS2 is involved in the inflammatory response in lung diseases. For example, ETS2 has been implicated in pulmonary fibrosis[20] and shown to elevate the expression of granulocyte-macrophage colony-stimulating factor in non-small lung carcinoma cells.[21] Neutrophil recruitment is a critical process in response to bacterial infections in the early stage, but excessive and inappropriate recruitment results in tissue damage.[4] In the current study, we found that downregulation of ETS2 reduced neutrophil accumulation, MPO activity, NET formation, TNF-α, and IL-6 levels. ETS2 downregulation may enhance neutrophil recruitment in ARDS

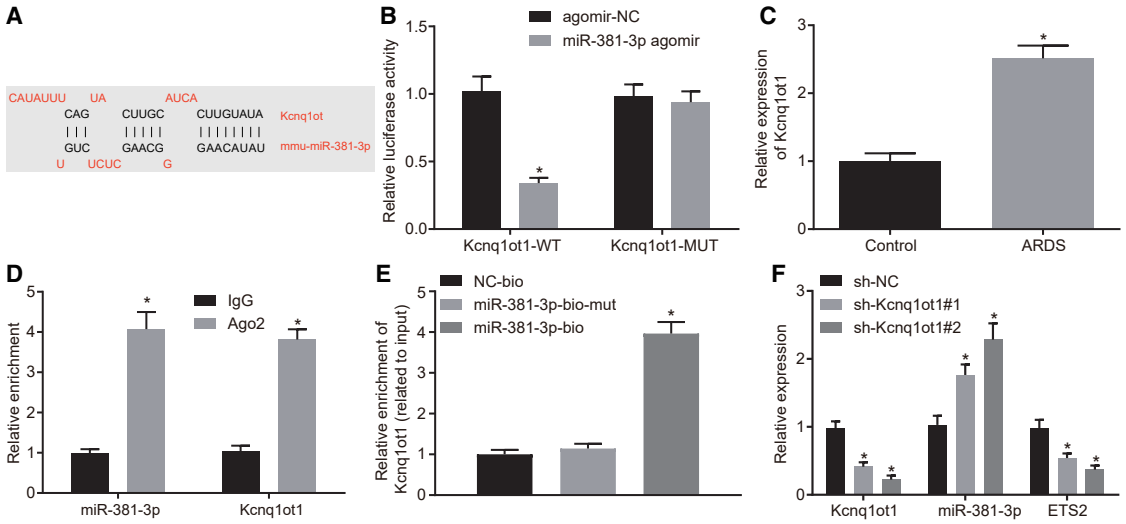

Figure 4. Kcnq1ot1 Competitively Binds to miR-381-3p to Promote ETS2 Expression

(A) Binding sites of Kcnq1ot1 to miR-381-3p predicted by the DIANA TOOLS database. (B) Binding of Kcnq1ot1 to miR-381-3p verified by dual-luciferase reporter assay (*$p < 0.05$ versus the agomir-NC group). (C) Expression of Kcnq1ot1 in BALF neutrophils in ARDS mouse models and mice in the control group as determined by qRT-PCR (*$p < 0.05$ versus the control group). (D) Binding of Kcnq1ot1 to miR-381-3p confirmed by RIP assay (*$p < 0.05$ versus the IgG group). (E) Binding of Kcnq1ot1 to miR-381-3p analyzed by RNA pull-down (*$p < 0.05$ versus the miR-183-5p-bio-mut group). (F) Expression of Kcnq1ot1, miR-381-3p, and ETS2 in BALF neutrophils of ARDS mouse models as determined by qRT-PCR (*$p < 0.05$ versus the sh-NC group). The measurement data are presented as mean ± SD. Comparison between two groups was analyzed by an unpaired t test. Comparisons among multiple groups were performed with one-way ANOVA, followed by Tukey's *post hoc* test. n = 8. The cell experiments were repeated three times.

mice on the grounds that a previous study showed that alleviation of lung injury was commonly associated with increased NET formation induced by pulmonary neutrophil recruitment.[7] Moreover, ETS2 downregulation may reduce inflammation because activated neutrophils produce proinflammatory cytokines such as TNF-α and ILs.[1] Our result also agrees with a previous study that ETS2 is involved in the modulation of inflammatory cytokines including ILs and TNF-α.[22] Collectively, our results strongly suggest that ETS2 is involved in acute neutrophil inflammation, which is one of the hallmarks of ARDS.[3]

Target genes of miR-381-3p are known to be involved in cellular processes and cellular macromolecule metabolism.[23] Notably, miR-381-3p mediates antigen-presenting ability in dendritic cells and anti-tuberculosis cellular immune responses by targeting CD1c.[24] In this study, we revealed that miR-381-3p directly targeted 3′ UTR of ETS2 and reduced the expression of ETS2. Therefore, miR-381-3p may inhibit inflammation in LPS-induced ARDS mice by targeting ETS2.

Furthermore, we found that Kcnq1ot1 bound to miR-381-3p to promote ETS2 expression. Kcnq1ot1 was demonstrated to serve as a competing endogenous (ceRNA) for miRNAs, such as sponging miR-214-3p to regulate caspase-1.[25] Inhibition of Kcnq1ot1 reduces inflammation in myocardial ischemia/reperfusion injury by targeting AdipoR1 via the p38 MAPK/nuclear factor κB (NF-κB) signaling pathway.[26,27] These results from previous studies agree with the idea that lncRNA Kcnq1ot1 promotes inflammatory response in ARDS mice. Our results further suggested that the effect of Kcnq1ot1 may work through sponging miR-381-3p and enhancing ETS2 expression. Conversely, Kcnq1ot1 silencing may attenuate the inflammatory response in ARDS.

In conclusion, we provide evidence that the Kcnq1ot1/miR-381-3p/ETS2 axis regulates neutrophil inflammatory response in LPS-induced ARDS mice. This study identifies the Kcnq1ot1/miR-381-3p/ETS2 axis as a novel biomarker for ARDS, which will ultimately provide new insights for prediction, prognosis, and treatment for patients with ARDS.

MATERIALS AND METHODS

Ethics Statement

All animal procedures were conducted in accordance with the *Guide for the Care and Use of Laboratory Animals*, published by the NIH (publication no. 85-23, revised 1996).[28] All animal experiments were approved by the Animal Care Committee at Zhejiang Provincial People's Hospital, People's Hospital of Hangzhou Medical College.

In Silico Analysis

ARDS-related expression dataset GSE76293 and its annotation probe were obtained through the GEO database (GEO: GSE76293). Differential gene expression analysis was performed using the R software. Differentially expressed genes were defined as $|\log_2$ fold change (FC)$| > 1$ and $p < 0.05$.

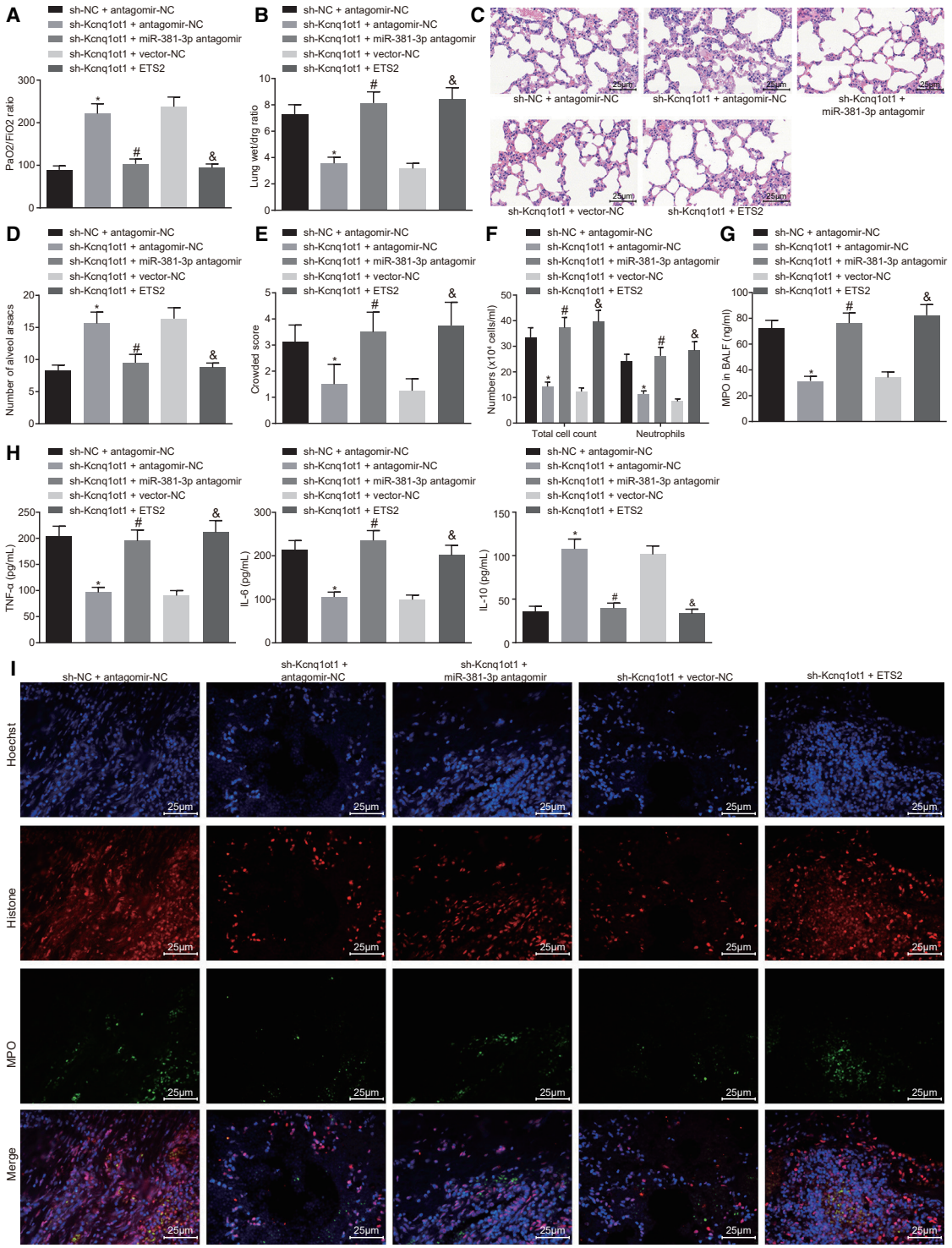

Figure 5. Kcnq1ot1/miR-381-3p/ETS2 Axis Regulates Inflammatory Response in ARDS Mouse Models

(A) Ratio of PaO_2/FiO_2. (B) Lung wet weight to dry weight ratio. (C) H&E staining to observe pathological changes of lung parenchymal (original magnification, ×400). (D) Number of alveolar sacs. (E) Lung parenchymal score. (F) Total cells and neutrophils in the BALF of mice. (G) MPO activity in BALF of mice. (H) ELISA was used to

(legend continued on next page)

Mouse Models Simulating ARDS

In total, 74 male specific pathogen-free (SPF) C57BL/6 mice (12 weeks old, weighing 18–23 g) were purchased from the Animal Experimental Research Center, Zhejiang Chinese Medical University (Hangzhou, Zhejiang, China). The mice were acclimatized for 1 week before they were weighed. 66 mice were randomly selected to establish models of ARDS. The mice were anesthetized by intraperitoneal injection of sodium pentobarbital (50 mg/kg, WS20060401, Sinopharm Chemical, China). Then, mice were fixed in the supine position to expose the skin of the neck, which was disinfected with 75% ethanol. The skin was cut open to separate the subcutaneous tissue layer by layer and expose the trachea. A micro-syringe was inserted into the trachea through the tracheal cartilage ring gap toward the heart end. If there was no resistance to pull back, 5 mg/kg LPS (*Escherichia coli* O111:B4 dissolved in saline, Sigma, St. Louis, MO, USA) was injected. Immediately after the operation, the mice were set upright and rotated, so that the LPS was evenly distributed in the lungs. The mice were supplied with oxygen, and the oxygen concentration was maintained at 2 L/min until they were awake. Then they were returned to the cage for routine feeding. There were 56 successfully established mouse models, with a success rate of 84.85%.[29,30]

Animal Grouping

Mice were randomly assigned into eight groups (n = 8 per group): control group (intratracheal instillation of 0.9% normal saline); ARDS group (intratracheal instillation of 5 mg/kg LPS); sh-NC group (intratracheal instillation of 5 mg/kg LPS 1 h before intravenous injection of sh-NC through caudal veins); sh-ETS2 group (5′-AGAAAU GGAAUCCAAGCCUGUUGGC-3′; 5′-GCCAACAGGCUUGGAU UCC AUUUCU-3′) (intratracheal instillation of 5 mg/kg LPS 1 h before intravenous injection of sh-ETS2 through caudal veins); sh-Kcnq1ot1 (5′-ACCCAACAACTCTGGAACATA-3′; 5′-TATGTT CCAGAGTTGTTGGG-3′) + antagomir-NC group (intratracheal instillation of 5 mg/kg LPS 1 h before intravenous injection of sh-Kcnq1ot1 + antagomir-NC through caudal veins); sh-Kcnq1ot1 + miR-381-3p antagomir group (intratracheal instillation of 5 mg/kg LPS 1 h before intravenous injection of sh-Kcnq1ot1 + miR-381-3p antagomir through caudal veins); sh-Kcnq1ot1 + vector-NC group (intratracheal instillation of 5 mg/kg LPS 1 h before intravenous injection of sh-Kcnq1ot1 + vector-NC through caudal veins); and sh-Kcnq1ot1 + ETS2 group (intratracheal instillation of 5 mg/kg LPS 1 h before intravenous injection of sh-Kcnq1ot1 + ETS2 through caudal veins). Lentiviruses of sh-Kcnq1ot1, sh-ETS2, and overexpressed ETS2 were purchased from Shanghai GenePharma (Shanghai, China). Lentivirus (1×10^9 transducing units [TU]) was dissolved in 50 μL of normal saline and then injected through the caudal vein.[31] miR-381-3p antagomir (miR30017081-4-5) and antagomir-NC (miR3N0000002-4-5) (100 nmol/L) were injected through the caudal vein (Guangzhou RiboBio, Guangzhou, Guangdong, China). Blood samples were collected from abdominal aorta 48 h after LPS injection. In addition, BALF was collected by bronchoalveolar lavage (BAL) in all groups.[29,30] Total and differential white blood cell counts were determined in BALF by an automated hematology analyzer (Sysmex, Kobe, Japan).[32]

Arterial Blood Gas Analysis and Lung Wet Weight to Dry Weight Ratio

PaO_2 and $PaCO_2$ were measured using an automatic blood gas analyzer (ABL800 FLEX, Radiometer, Bronshoj, Denmark). The oxygenation index was calculated by the ratio of PaO_2 to FiO_2. Lungs were excised and weighed for wet weight immediately after the mice were sacrificed. Lungs were then dehydrated in an oven at 60°C, and the dry weight was measured 72 h later. The ratio of dry weight to wet weight of the lung was then calculated.[32]

Histological Evaluation of Lung Injury

Lower right lung lobe was cut into thin sections (5 μm). The number of alveolar sacs was determined after H&E staining by investigators blinded to experimental groups. Three lung sections of each mouse were evaluated. Three high-power fields (×100) were randomly selected in each section for observation. The average number of alveolar sacs per mouse was determined by the sum from all fields divided by 9. The crowded area was defined as thickened septa in lung parenchyma where alveolar sacs were partly or completely collapsed under H&E-stained sections. A scoring system was used to quantify the crowded area by investigators blinded to experimental groups, defined as follows: 0, no crowded area; 1, 15% of the total high-power field was a crowded area; 2, 15%–25% crowded area; 3, 25%–50% crowded area; 4, 50%–75% crowded area; 5, ≥75%–100% of the area was crowded.[28]

MPO Activity Assay

BALF (100 μL) was mixed with substrate solution containing citrate buffer (10 mM citric acid + 10 mM sodium citrate), 5 mg *o*-phenylenediamine dihydrochloride (OPD; Sigma, St. Louis, MO, USA), and 5 μL of H_2O_2 (8.8 mM). A standard curve was established by mixing 100 μL of 500 ng/mL type II horseradish peroxidase (HRP; Sigma, St. Louis, MO, USA) and 100 μL of substrate solution. 4 N H_2SO_4 was used as the stop solution. Samples were read by a spectrophotometer (Epoch, BioTek, Winooski, VT, USA) at 492 nm.[6]

Immunofluorescence

Paraffin-embedded lung sections (5 μm) were dewaxed, permeabilized, mounted, and then incubated with histone H3 goat polyclonal immunoglobulin (Ig)G (C-16) antibody (1:200; Santa Cruz, Santa Cruz, CA, USA) and MPO anti-rabbit antibody (1:400; Dako, Glostrup, Denmark) at 4°C overnight. Then, Alexa Fluor 488 donkey

detect the content of TNF-α, IL-6, and IL-10 in BALF of mice. (l) NETs formation by immunofluorescence (original magnification, ×400). *$p < 0.05$ versus the sh-NC + antagomir-NC group; #$p < 0.05$ versus the sh-Kcnq1ot1 + antagomir-NC group; &$p < 0.05$ versus the sh-Kcnq1ot1 + vector-NC group. The measurement data are presented as mean ± SD. Comparisons among multiple groups were performed with one-way ANOVA, Brown-Forsythe's and Welch's ANOVA tests, and a Kruskal-Wallis test. n = 8.

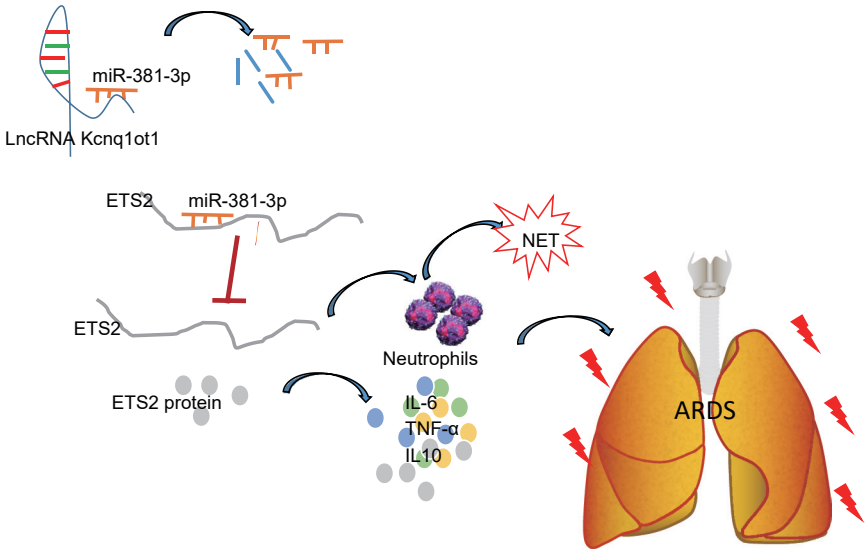

Figure 6. Kcnq1ot1 Reverses the Inhibitory Effect of miR-381-3p on the Expression of ETS2 by Competitively Binding to miR-381-3p, Thereby Promoting Neutrophil Recruitment and Inflammatory Cytokine Expression in BALF in Mouse Models of ARDS

anti-rabbit antibody and Alexa Fluor 568 donkey anti-goat secondary antibody (1:200; Invitrogen, Carlsbad, CA, USA) were added for a 1-h incubation at room temperature. Hoechst 33342 (100 ng/mL, Invitrogen) was used to stain DNA. The formation of NETs was observed under a confocal microscope.[6]

ELISA

The levels of IL-6, TNF-α, and IL-10 in BALF were simultaneously measured by a Luminex Multiplex Assay kit (Thermo Fisher Scientific, Waltham, MA, USA). Cytokine quantification was performed using a Luminex 100/200 luminometer (Luminex, Austin, TX, USA) and xPONENT Solutions software (Luminex).[33]

Polymorphonuclear Leukocyte Isolation and Culture

Neutrophils were isolated from mouse BALF by Histopaque centrifugation. Polymorphonuclear leukocytes (PMNs) were collected, isolated, and purified by flow cytometry (Galios; Beckman Coulter, Roissy, France). Neutrophils (>95% pure) were cultured in RPMI 1640 medium (Sigma, St. Louis, MO, USA) containing 10% fetal bovine serum (FBS) (Thermo Fisher Scientific) for subsequent experiments.[34,35]

RNA Isolation and qRT-PCR

After extraction of total RNA from peripheral blood or neutrophils with a TRIzol kit (15596026, Ambion, Austin, TX, USA), RNAs (5 μg) were reverse transcribed to synthesize cDNA according to instructions in the GoScript reverse transcription system (A5001, Promega, Madison, WI, USA). Expression of miR-381-3p was determined using a TaqMan miRNA assay (Ambion). U6 was used as an internal reference. Expression of Kcnq1ot1 and ETS2 was determined by PrimeScript qRT-PCR kits (Roche, Basel, Switzerland). β-Actin was used as an internal reference. All primers were synthesized by Takara (Dalian, Liaoning, China) (Table 1). Changes in mRNA expressions were calculated by relative quantification ($2^{-\Delta\Delta Ct}$ method), where $\Delta\Delta Ct = \Delta Ct_{\text{experimental group}} - \Delta Ct_{\text{control group}}$ and $\Delta Ct = Ct_{\text{target gene}} - Ct_{\text{internal reference gene}}$. The Ct value refers to the fractional cycle at which the fluorescence intensity equals the threshold fluorescence, at which point the amplification is in logarithmic growth. The experiment was repeated three times.[25]

Western Blot Analysis

An equal amount (10–30 μg) of protein extract (from peripheral blood or neutrophils) was separated by SDS-PAGE with gradient acrylamide (8%–10%). After electrophoresis, separated proteins were electrophoretically transferred to a polyvinylidene fluoride (PVDF) membrane (Amersham Biosciences, Amersham, UK). Nonspecific binding sites in the PVDF membrane were blocked. Then, membranes were incubated with rabbit anti-EST2 (1 μg/mL, ab153652) overnight at 4°C, followed by incubation with HRP-labeled goat anti-rabbit secondary antibody (1:5,000, ab6721) for 1 h. An enhanced chemiluminescence detection kit (BB-3501, Amerham) was used to visualize images, which were obtained with a Bio-Rad image analysis system (Bio-Rad, Hercules, CA, USA) and analyzed by Quantity One v4.6.2 software. Relative protein level was determined as the gray value of the corresponding protein band divided by the gray value of the β-actin protein band. The experiment was repeated three times.

Dual-Luciferase Reporter Assay

Synthetic EST2 3′ UTR gene fragments were introduced into pMIR-reporter (Beijing Huayueyang Biotechnology, Beijing, China) through endonuclease sites SpeI and HindIII. Mutation sites of the complementary sequence in the seed sequence were designed on EST2 WT. Target fragments were inserted into the pMIR-reporter plasmid using T4 DNA ligase after restriction endonuclease digestion. The correctly sequenced luciferase reporter plasmids EST2 3′ UTR-WT and EST2 3′ UTR-MUT were co-transfected in HEK293T cells (CRL-1415, Shanghai Xinyu Biotechnology, Shanghai, China) with miR-381-3p agomir (miR40017081-4-5, Guangzhou RiboBio, Guangzhou, Guangdong, China) or agomir-NC (miR4N0000002-4-5, Guangzhou RiboBio, Guangzhou, Guangdong, China). Cells were collected and lysed for 48 h after transfection, and then luciferase activity was examined in a GloMax 20/20 luminometer (Promega) using a luciferase assay kit (RG005, Beyotime Institute of Biotechnology, Shanghai, China). The experiment was repeated three times. The putative binding sites of miR-381-3p recognized by Kcnq1ot1 were also examined by the same method.

Table 1. Primer Sequences for RT-PCR

Gene	Primer Sequence
ETS2	Forward: 5′-CACGGGCCTAATCCTCAGTC-3′
	Reverse: 5′-GAAGGTTTTGTAATTTGGCC-3′
Kcnq1ot1	Forward: 5′-CGCGATCCTCCTCAGTGTTT-3′
	Reverse: 5′-CATATCGCCGACCACCATGA-3′
miR-381-3p	Forward: 5′-TCAGACGACAACCGTCTGTG-3′
	Reverse: 5′-AAAATTGAGCACCAACGGGC-3′
U6	Forward: 5′-CTCGCTTCGGCAGCACA-3′
	Reverse: 5′-AACGCTTCACGAATTTGCGT-3′
β-Actin	Forward: 5′-AGTGTGACGTTGACATCCGT-3′
	Reverse: 5′-GCCAGAGCAGTAATCTCCTTCT-3′

ETS2, E26 transformation-specific proto-oncogene 2.

RIP Assay

Neutrophils were collected after trypsinization. Lysis buffer containing RNase (Life Technologies, Gaithersburg, MD, USA) and protease inhibitor cocktail (Roche) was added to lyse cells. The lysate was centrifuged at 12,000 × *g* for 30 min and supernatant was collected. Protein G-agarose beads were incubated with Ago2 antibody (P10502500, Otwo Biotech, Shenzhen, Guangdong, China) and IgG (Sigma, St. Louis, MO, USA) for 2 h at 4°C. Then, cell lysate supernatant was added and incubated overnight at 4°C. RNA was extracted from magnetic beads using TRIzol reagent (Invitrogen). mRNA expressions of Kcnq1ot1 and miR-381-3p were detected by qRT-PCR.

RNA Pull-Down Assay

Neutrophils were transfected with 50 nM biotinylated bio-miR-381-3p-WT, bio-miR-381-3p-bio-mut, or the corresponding NC-bio. After 48 h, harvested cells were incubated in a specific lysis buffer (Ambion) for 10 min and centrifuged at 14,000 × *g*. Supernatant was collected and incubated with M-280 streptavidin magnetic beads (S3762, Sigma) pre-coated with RNase-free BSA and yeast tRNA (TRNABAK-RO, Sigma, St. Louis, MO, USA) for 3 h at 4°C. Beads were then washed twice with pre-chilled lysis buffer, three times with low-salt buffer, and once with high-salt buffer. Bound RNA was purified by TRIzol. mRNA expression of Kcnq1ot1 was detected by qRT-PCR.

Statistical Analysis

Statistical analysis was performed using SPSS version 21.0 (IBM Software, New York, NY, USA). The measurement data were presented as mean ± SD. The normal distribution was checked by a Kolmogorov-Smirnov test, and the homogeneity of variance was checked by Levene's test. For comparisons between two groups, an unpaired t test was performed when data were in line with normal distribution and homogeneity of variance, while a Welch's correction t test was conducted when data were consistent with normal distribution yet inconsistent with homogeneity of variance, and a Mann-Whitney test was carried out for data with skewed distribution. For comparisons among multiple groups, one-way ANOVA with a Tukey's *post hoc* test was performed when data conformed to normal distribution and homogeneity of variance, while Brown-Forsythe's and Welch's ANOVA tests were conducted when data were in accordance with normal distribution yet disobeyed from homogeneity of variance (Tamhane T2 for pairwise comparisons), and a Kruskal-Wallis test was used for data with skewed distribution (Dunn's multiple comparisons test for pairwise comparisons). Statistical significance was defined as $p < 0.05$.

SUPPLEMENTAL INFORMATION

Supplemental Information can be found online at https://doi.org/10.1016/j.omtn.2019.10.036.

AUTHOR CONTRIBUTIONS

X.J., T.Z., L.L., and X.C. and designed the study. M.Y., Q.L., D.W., and R.S. collated the data, carried out data analyses, and produced the initial draft of the manuscript. X.J. and M.Y. contributed to drafting the manuscript. All authors have read and approved the final submitted manuscript.

CONFLICTS OF INTEREST

The authors declare no competing interests.

ACKNOWLEDGMENTS

We would like show sincere appreciation to the reviewers for critical comments on this article.

REFERENCES

1. Prabhakaran, P. (2010). Acute respiratory distress syndrome. Indian Pediatr. *47*, 861–868.
2. Bellani, G., Laffey, J.G., Pham, T., Fan, E., Brochard, L., Esteban, A., Gattinoni, L., van Haren, F., Larsson, A., McAuley, D.F., et al.; LUNG SAFE Investigators; ESICM Trials Group (2016). Epidemiology, patterns of care, and mortality for patients with acute respiratory distress syndrome in intensive care units in 50 countries. JAMA *315*, 788–800.
3. Villar, J., Blanco, J., and Kacmarek, R.M. (2016). Current incidence and outcome of the acute respiratory distress syndrome. Curr. Opin. Crit. Care *22*, 1–6.
4. Sabroe, I., and Whyte, M.K. (2007). Toll-like receptor (TLR)-based networks regulate neutrophilic inflammation in respiratory disease. Biochem. Soc. Trans. *35*, 1492–1495.
5. Zhang, Y., Liu, H., Yao, J., Huang, Y., Qin, S., Sun, Z., Xu, Y., Wan, S., Cheng, H., Li, C., et al. (2016). Manipulating the air-filled zebrafish swim bladder as a neutrophilic inflammation model for acute lung injury. Cell Death Dis. *7*, e2470.
6. Sercundes, M.K., Ortolan, L.S., Debone, D., Soeiro-Pereira, P.V., Gomes, E., Aitken, E.H., Condino-Neto, A., Russo, M., D' Império Lima, M.R., Alvarez, J.M., et al. (2016). Targeting neutrophils to prevent malaria-associated acute lung injury/acute respiratory distress syndrome in mice. PLoS Pathog. *12*, e1006054.
7. Müller-Redetzky, H. (2015). Targeting neutrophil extracellular traps in acute lung injury: a novel therapeutic approach in acute respiratory distress syndrome? Anesthesiology *122*, 725–727.
8. Zabuawala, T., Taffany, D.A., Sharma, S.M., Merchant, A., Adair, B., Srinivasan, R., Rosol, T.J., Fernandez, S., Huang, K., Leone, G., and Ostrowski, M.C. (2010). An *Ets2*-driven transcriptional program in tumor-associated macrophages promotes tumor metastasis. Cancer Res. *70*, 1323–1333.
9. Liu, X., Zhang, C., Zhang, Z., Zhang, Z., Ji, W., Cao, S., Cai, X., Lei, D., and Pan, X. (2017). E26 transformation-specific transcription factor ETS2 as an oncogene

promotes the progression of hypopharyngeal cancer. Cancer Biother. Radiopharm. *32*, 327–334.

10. Furukawa, T., Tanji, E., Xu, S., and Horii, A. (2008). Feedback regulation of *DUSP6* transcription responding to MAPK1 via ETS2 in human cells. Biochem. Biophys. Res. Commun. *377*, 317–320.

11. Hu, W.W., Chen, P.C., Chen, J.M., Wu, Y.M., Liu, P.Y., Lu, C.H., Lin, Y.F., Tang, C.H., and Chao, C.C. (2017). Periostin promotes epithelial-mesenchymal transition via the MAPK/miR-381 axis in lung cancer. Oncotarget *8*, 62248–62260.

12. Zhang, Y., Wang, X., Liu, Z., and Yu, L. (2018). Dexmedetomidine attenuates lipopolysaccharide induced acute lung injury by targeting NLRP3 via miR-381. J. Biochem. Mol. Toxicol. *32*, e22211.

13. Gao, X., Ge, J., Li, W., Zhou, W., and Xu, L. (2018). lncRNA KCNQ1OT1 ameliorates particle-induced osteolysis through inducing macrophage polarization by inhibiting miR-21a-5p. Biol. Chem. *399*, 375–386.

14. Pandey, R.R., Mondal, T., Mohammad, F., Enroth, S., Redrup, L., Komorowski, J., Nagano, T., Mancini-Dinardo, D., and Kanduri, C. (2008). Kcnq1ot1 antisense noncoding RNA mediates lineage-specific transcriptional silencing through chromatin-level regulation. Mol. Cell *32*, 232–246.

15. Ren, K., Xu, R., Huang, J., Zhao, J., and Shi, W. (2017). Knockdown of long non-coding RNA KCNQ1OT1 depressed chemoresistance to paclitaxel in lung adenocarcinoma. Cancer Chemother. Pharmacol. *80*, 243–250.

16. Pan, C., Liu, L., Xie, J.F., and Qiu, H.B. (2018). Acute respiratory distress syndrome: challenge for diagnosis and therapy. Chin. Med. J. (Engl.) *131*, 1220–1224.

17. José, R., Williams, A., Sulikowski, M., Brealey, D., Brown, J., and Chambers, R. (2015). Regulation of neutrophilic inflammation in lung injury induced by community-acquired pneumonia. Lancet *385* (*Suppl 1*), S52.

18. Kim, J.H., Suk, M.H., Yoon, D.W., Lee, S.H., Hur, G.Y., Jung, K.H., Jeong, H.C., Lee, S.Y., Lee, S.Y., Suh, I.B., et al. (2006). Inhibition of matrix metalloproteinase-9 prevents neutrophilic inflammation in ventilator-induced lung injury. Am. J. Physiol. Lung Cell. Mol. Physiol. *291*, L580–L587.

19. Dong, Z., Yang, P., Qiu, X., Liang, S., Guan, B., Yang, H., Li, F., Sun, L., Liu, H., Zou, G., and Zhao, K. (2019). KCNQ1OT1 facilitates progression of non-small-cell lung carcinoma via modulating miRNA-27b-3p/HSP90AA1 axis. J. Cell. Physiol. *234*, 11304–11314.

20. Baran, C.P., Fischer, S.N., Nuovo, G.J., Kabbout, M.N., Hitchcock, C.L., Bringardner, B.D., McMaken, S., Newland, C.A., Cantemir-Stone, C.Z., Phillips, G.S., et al. (2011). Transcription factor ets-2 plays an important role in the pathogenesis of pulmonary fibrosis. Am. J. Respir. Cell Mol. Biol. *45*, 999–1006.

21. Lu, Z., Kim, K.A., Suico, M.A., Uto, A., Seki, Y., Shuto, T., Isohama, Y., Miyata, T., and Kai, H. (2003). ETS2 is involved in protein kinase C-activated expression of granulocyte-macrophage colony-stimulating factor in human non-small lung carcinoma cell line, A549. Biochem. Biophys. Res. Commun. *303*, 190–195.

22. Cheng, C., Tempel, D., Den Dekker, W.K., Haasdijk, R., Chrifi, I., Bos, F.L., Wagtmans, K., van de Kamp, E.H., Blonden, L., Biessen, E.A., et al. (2011). Ets2 determines the inflammatory state of endothelial cells in advanced atherosclerotic lesions. Circ. Res. *109*, 382–395.

23. Tang, G., and Long, D.-X. (2018). Bioinformatics analysis of target gene prediction and related signaling pathways of hsa-miR-381-3p. Life Sci. Res *22*, 222–228.

24. Wen, Q., Zhou, C., Xiong, W., Su, J., He, J., Zhang, S., Du, X., Liu, S., Wang, J., and Ma, L. (2016). miR-381-3p regulates the antigen-presenting capability of dendritic cells and represses antituberculosis cellular immune responses by targeting CD1c. J. Immunol. *197*, 580–589.

25. Yang, F., Qin, Y., Lv, J., Wang, Y., Che, H., Chen, X., Jiang, Y., Li, A., Sun, X., Yue, E., et al. (2018). Silencing long non-coding RNA Kcnq1ot1 alleviates pyroptosis and fibrosis in diabetic cardiomyopathy. Cell Death Dis. *9*, 1000.

26. Yang, M., Chen, J., Zhao, J., and Meng, M. (2014). Etanercept attenuates myocardial ischemia/reperfusion injury by decreasing inflammation and oxidative stress. PLoS ONE *9*, e108024.

27. Li, X., Dai, Y., Yan, S., Shi, Y., Han, B., Li, J., Cha, L., and Mu, J. (2017). Down-regulation of lncRNA KCNQ1OT1 protects against myocardial ischemia/reperfusion injury following acute myocardial infarction. Biochem. Biophys. Res. Commun. *491*, 1026–1033.

28. Sun, C.K., Lee, F.Y., Kao, Y.H., Chiang, H.J., Sung, P.H., Tsai, T.H., Lin, Y.C., Leu, S., Wu, Y.C., Lu, H.I., et al. (2015). Systemic combined melatonin-mitochondria treatment improves acute respiratory distress syndrome in the rat. J. Pineal Res. *58*, 137–150.

29. Chen, Y., Wang, D., Zhao, Y., Huang, B., Cao, H., and Qi, D. (2018). p300 promotes differentiation of Th17 cells via positive regulation of the nuclear transcription factor RORγt in acute respiratory distress syndrome. Immunol. Lett. *202*, 8–15.

30. D'Alessio, F.R., Craig, J.M., Singer, B.D., Files, D.C., Mock, J.R., Garibaldi, B.T., Fallica, J., Tripathi, A., Mandke, P., Gans, J.H., et al. (2016). Enhanced resolution of experimental ARDS through IL-4-mediated lung macrophage reprogramming. Am. J. Physiol. Lung Cell. Mol. Physiol. *310*, L733–L746.

31. Liu, S., Tang, J., Huang, L., Xu, Q., Ling, X., and Liu, J. (2015). Cordyceps militaris alleviates severity of murine acute lung injury through miRNAs-mediated CXCR2 inhibition. Cell. Physiol. Biochem. *36*, 2003–2011.

32. Wang, S., Li, Z., Chen, Q., Wang, L., Zheng, J., Lin, Z., and Li, W. (2018). NF-κB-induced microRNA-211 inhibits interleukin-10 in macrophages of rats with lipopolysaccharide-induced acute respiratory distress syndrome. Cell. Physiol. Biochem. *45*, 332–342.

33. Pedrazza, L., Cunha, A.A., Luft, C., Nunes, N.K., Schimitz, F., Gassen, R.B., Breda, R.V., Donadio, M.V., de Souza Wyse, A.T., Pitrez, P.M.C., et al. (2017). Mesenchymal stem cells improves survival in LPS-induced acute lung injury acting through inhibition of NETs formation. J. Cell. Physiol. *232*, 3552–3564.

34. Grégoire, M., Tadié, J.M., Uhel, F., Gacouin, A., Piau, C., Bone, N., Le Tulzo, Y., Abraham, E., Tarte, K., and Zmijewski, J.W. (2017). Frontline Science: HMGB1 induces neutrophil dysfunction in experimental sepsis and in patients who survive septic shock. J. Leukoc. Biol. *101*, 1281–1287.

35. Grégoire, M., Uhel, F., Lesouhaitier, M., Gacouin, A., Guirriec, M., Mourcin, F., Dumontet, E., Chalin, A., Samson, M., Berthelot, L.L., et al. (2018). Impaired efferocytosis and neutrophil extracellular trap clearance by macrophages in ARDS. Eur. Respir. J. *52*, 1702590.

OMTN, Volume *19*

Supplemental Information

Kcnq1ot1/miR-381-3p/ETS2 Axis Regulates Inflammation in Mouse Models of Acute Respiratory Distress Syndrome

Xiaohui Jiang, Meihong Yu, Taiping Zhu, Lulu Lou, Xu Chen, Qian Li, Danhong Wei, and Renhua Sun

Supplementary Table 1. The differential analysis results of allgenes

logFC	AveExpr	t	*p*. Value	adj.*p*.Val	B	
ETS2	1.552580906	7.679311155	14.0513358	3.84E-13	5.22E-09	19.63873215
CDK5RAP2	2.251367569	9.157797722	13.85036019	5.25E-13	5.22E-09	19.35967902
GRB10	2.676412417	8.210899219	13.48869855	9.28E-13	5.22E-09	18.84703325
CD177	3.894762431	11.29034042	13.46425107	9.64E-13	5.22E-09	18.81188505
GYG1	2.08718041	10.47582225	13.19433405	1.49E-12	6.45E-09	18.41958226
P2RY10	-1.369432045	5.778241085	-12.85788829	2.58E-12	9.31E-09	17.91949293
IRAK3	2.283897424	9.287247816	12.54237783	4.37E-12	1.35E-08	17.43903951
UPP1	1.251842917	13.18386306	12.14572019	8.58E-12	2.32E-08	16.81877606
ZDHHC20	1.893601573	6.979373071	11.8106408	1.54E-11	3.48E-08	16.2802938
BTBD11	-1.249885455	5.508767245	-11.78563274	1.61E-11	3.48E-08	16.23956117
MCEMP1	1.80846951	12.37926579	11.67186386	1.97E-11	3.87E-08	16.05329084
MAPK14	1.357129639	10.6680844	10.88942309	8.14E-11	1.47E-07	14.72828621
HLTF	2.497239851	7.162810981	10.72292997	1.11E-10	1.85E-07	14.43617587
MYBPH	-1.315421286	7.039624685	-10.50538689	1.68E-10	2.51E-07	14.04897141
EXOSC4	1.715363243	9.982438778	10.48699722	1.74E-10	2.51E-07	14.01594998
NLRC4	1.022665451	7.631234458	10.12363167	3.51E-10	4.47E-07	13.35408957
VNN1	2.344156465	9.098535753	9.993039545	4.53E-10	5.45E-07	13.11180998
SLC25A45	-1.047842806	7.673991622	-9.959747473	4.84E-10	5.51E-07	13.04966837
GADD45A	1.928097865	10.1988178	9.913055763	5.30E-10	5.74E-07	12.96225657
MTHFD2	1.191611014	7.84827399	9.824621486	6.32E-10	6.22E-07	12.79586707
NOV	-1.20153325	5.437281729	-9.754043035	7.28E-10	6.85E-07	12.66228988
AGFG1	1.640278139	9.350338198	9.581717728	1.03E-09	9.28E-07	12.33320718
PECR	1.049434944	7.447300132	9.483437568	1.26E-09	1.09E-06	12.14364805
MAP7	-1.558343962	5.991078214	-9.370332664	1.58E-09	1.32E-06	11.92379793
STOM	1.605393993	8.003100851	9.14836773	2.50E-09	2.00E-06	11.48703704
TDRD9	3.493719906	8.058648658	9.105257589	2.73E-09	2.11E-06	11.4013892
SMARCD3	1.022370653	8.845440295	9.087939867	2.83E-09	2.12E-06	11.36690839

PCMT1	1.030177986	10.06286801	9.034275719	3.17E-09	2.29E-06	11.2597848
LHX4	1.303179406	6.559325637	8.997506066	3.42E-09	2.39E-06	11.18614591
IL1R2	1.064284646	12.19333476	8.924208765	3.99E-09	2.62E-06	11.03877
CEBPA	1.21352408	8.635365238	8.912001827	4.10E-09	2.62E-06	11.01415053
GRINA	1.207995139	11.57778369	8.910104508	4.11E-09	2.62E-06	11.010322
PLEKHO1	-2.007154007	10.47307762	-8.845949944	4.71E-09	2.70E-06	10.88056008
HSH2D	-1.786235479	8.692095826	-8.830030482	4.87E-09	2.70E-06	10.84826831
CD44	1.102242986	7.795070049	8.779111719	5.42E-09	2.94E-06	10.74473558
TLR5	1.939188771	10.14244174	8.749919147	5.77E-09	3.05E-06	10.68520888
RP1-193H18.2	2.040529069	6.763274764	8.697257751	6.46E-09	3.08E-06	10.57751385
SRPK1	1.421093535	9.308777663	8.690598571	6.55E-09	3.08E-06	10.56386682
CYP1B1	2.347968035	7.156156208	8.616008163	7.68E-09	3.51E-06	10.41056415
IDNK	1.753171212	8.689818411	8.577557084	8.34E-09	3.69E-06	10.33122119
IL18R1	2.696613865	9.183402655	8.522913405	9.39E-09	4.07E-06	10.21809515
AK025288	1.355238108	10.40626991	8.456899439	1.08E-08	4.60E-06	10.08085032
SORT1	1.106631243	8.117531892	8.422121584	1.17E-08	4.86E-06	10.00829116
TPST2	1.277946927	10.82268172	8.40910711	1.20E-08	4.91E-06	9.981093017
FKBP5	2.124480649	8.012705793	8.372818973	1.30E-08	5.03E-06	9.905126519
TRPM2	1.848831934	7.752551764	8.361277571	1.33E-08	5.06E-06	9.880925299
MAP2K6	1.317446569	7.06605542	8.304071479	1.51E-08	5.64E-06	9.760683539
ARG1	2.770833434	6.763545186	8.261371035	1.66E-08	6.02E-06	9.670621081
RAB32	1.172583063	10.35276517	8.25899716	1.67E-08	6.02E-06	9.6656064
TIGD3	-2.301458009	9.096014506	-8.241330935	1.73E-08	6.11E-06	9.628261737
PKM	1.702982229	9.243544642	8.236870844	1.75E-08	6.11E-06	9.618826373
GAS7	1.115072351	9.065113116	8.212743501	1.84E-08	6.15E-06	9.567734648
RPGRIP1	-2.59097149	8.800049203	-8.194581999	1.92E-08	6.16E-06	9.529220324
HS3ST3B1	1.066197177	5.355882373	8.059842028	2.59E-08	7.78E-06	9.24198834
FUNDC1	-1.318114049	6.419590108	-8.031529523	2.75E-08	8.06E-06	9.181298671
MEF2C	-1.242135531	6.78695513	-7.981919455	3.08E-08	8.86E-06	9.074676747

METTL9	1.181020646	10.81363439	7.976982049	3.11E-08	8.86E-06	9.064045817
SNX3	1.397332583	9.526581667	7.923077306	3.51E-08	9.57E-06	8.947752404
CSF1R	-2.071697238	8.447566044	-7.920979265	3.52E-08	9.57E-06	8.943217642
MPEG1	-1.691594469	10.30212074	-7.914167106	3.58E-08	9.57E-06	8.92848929
ATP11B	1.263621955	7.972400964	7.844461486	4.18E-08	1.10E-05	8.777397024
CCDC146	-1.467166406	6.875479571	-7.837448852	4.25E-08	1.10E-05	8.76215792
LOC102723526	-1.397073719	8.628917144	-7.818336537	4.44E-08	1.12E-05	8.720589234
KCNE1	1.621025337	6.818895783	7.801303472	4.61E-08	1.12E-05	8.683498677
HP	2.204975601	9.934647786	7.795549698	4.67E-08	1.12E-05	8.670960077
RP11-44F14.8	-1.634831802	7.197646925	-7.793855466	4.69E-08	1.12E-05	8.667267109
CCDC153	-1.312611438	8.903412243	-7.771759386	4.93E-08	1.15E-05	8.619065962
CYSLTR1	-1.228330837	6.619906738	-7.758041103	5.08E-08	1.17E-05	8.589105254
SMA4	1.065295149	8.343198095	7.730242798	5.41E-08	1.22E-05	8.528311267
PNMA6A	-1.308113226	8.58399087	-7.716627379	5.58E-08	1.23E-05	8.498494503
LOC283588	-1.517599292	6.915786552	-7.706589089	5.71E-08	1.25E-05	8.47649444
CDKN2C	1.182059278	7.756680639	7.692043582	5.90E-08	1.25E-05	8.444590792
ASF1B	-1.497122757	7.876277813	-7.6170967	7.00E-08	1.40E-05	8.279727296
RPS6KA5	-1.300554861	7.004017194	-7.603247779	7.22E-08	1.42E-05	8.24917596
GALNT14	2.192178712	10.14068639	7.590803344	7.43E-08	1.43E-05	8.221699797
CASS4	-1.13683574	6.155957839	-7.589069089	7.46E-08	1.43E-05	8.217868981
HVCN1	-2.216065608	9.722262283	-7.584674482	7.54E-08	1.43E-05	8.208159774
NAIP	1.767800049	8.960480708	7.517849679	8.78E-08	1.62E-05	8.060184397
MS4A6A	1.076941493	9.273675476	7.473075058	9.73E-08	1.76E-05	7.960684417
FOXC1	1.505446003	7.272335283	7.462127681	9.98E-08	1.79E-05	7.936313875
GPX3	-1.978061222	6.239807604	-7.458575235	1.01E-07	1.79E-05	7.928401973
SORD	-1.385719743	7.447510583	-7.453879143	1.02E-07	1.79E-05	7.917940264
NHS	-1.624115111	6.361414458	-7.40769152	1.13E-07	1.96E-05	7.814881468
SAMSN1	1.368990135	6.720713002	7.376880713	1.21E-07	2.09E-05	7.745967525
SNRNP25	-1.482259155	8.45265499	-7.363999467	1.25E-07	2.12E-05	7.717117123

ARRB1	-1.346908212	8.138001595	-7.353020715	1.28E-07	2.15E-05	7.692509581
CCR3	-2.060902965	7.886530045	-7.290906995	1.48E-07	2.41E-05	7.552974739
PLAC8	2.399659531	10.55786074	7.259480108	1.59E-07	2.53E-05	7.482173201
PAG1	1.550239372	9.880277852	7.257225006	1.60E-07	2.53E-05	7.477087464
TBC1D8	2.320674431	7.797067531	7.223607139	1.73E-07	2.68E-05	7.401189275
C9orf91	-1.347242469	5.472976748	-7.187395959	1.89E-07	2.82E-05	7.319263266
ROGDI	1.317740531	8.609126866	7.11487307	2.23E-07	3.23E-05	7.154647531
MAST4	1.37377666	6.766536997	7.074627041	2.46E-07	3.50E-05	7.062988624
OPLAH	1.922216316	8.221221582	7.062011408	2.53E-07	3.56E-05	7.034212163
ESYT1	-1.600891344	9.931339839	-7.049859216	2.60E-07	3.59E-05	7.006472664
CLEC4D	1.817982434	10.11944442	7.026977663	2.75E-07	3.69E-05	6.95418796
OLAH	2.669610814	6.233351442	6.99688036	2.95E-07	3.87E-05	6.885308966
PPCDC	-1.370550972	9.974888924	-6.993165205	2.97E-07	3.87E-05	6.876798328
BCAT1	1.877652031	6.579976217	6.991148556	2.99E-07	3.87E-05	6.872177845
TSPAN13	-1.904569099	4.761768756	-6.976196078	3.10E-07	3.99E-05	6.837902393
MSMO1	1.473571417	8.478056188	6.937400044	3.39E-07	4.27E-05	6.748832891
BATF	1.72022774	9.405143807	6.91213347	3.60E-07	4.48E-05	6.690718488
GPR162	-2.015172653	8.856331118	-6.902362924	3.69E-07	4.56E-05	6.668223332
IDO1	-1.983738747	6.269685113	-6.894937079	3.75E-07	4.62E-05	6.651118146
METTL7B	3.384873816	5.302268283	6.883406022	3.86E-07	4.66E-05	6.624542495
ACBD6	1.544005962	8.616567845	6.810131069	4.59E-07	5.45E-05	6.455262811
ALPL	1.007957865	6.90025829	6.808462587	4.61E-07	5.45E-05	6.451400227
SULT1B1	1.477694997	8.454677432	6.802325159	4.68E-07	5.47E-05	6.437188829
RSBN1	1.085503674	8.182393458	6.757418471	5.20E-07	5.89E-05	6.333059565
PPIH	-1.144883052	7.540876394	-6.753992327	5.25E-07	5.89E-05	6.325104507
MAP3K14	-1.008328649	8.322623568	-6.724255468	5.63E-07	6.17E-05	6.255996967
ST3GAL4-AS1	1.507874767	10.0592043	6.71365009	5.78E-07	6.26E-05	6.23132339
AKT1	-1.188995747	7.175962512	-6.576642438	8.03E-07	8.20E-05	5.911313138
CARD6	1.219712507	11.23037446	6.559105774	8.38E-07	8.48E-05	5.870185937

FGL2	-1.228134979	10.81413755	-6.544823334	8.67E-07	8.69E-05	5.836663033
GPR84	2.831090476	7.27388796	6.53712103	8.83E-07	8.81E-05	5.818574411
SEL1L3	1.313216573	5.959041495	6.529361867	9.00E-07	8.91E-05	5.800345028
SLC37A3	1.486231266	7.340052793	6.52882512	9.01E-07	8.91E-05	5.799083728
LOC154761	1.619126958	6.652815368	6.517338202	9.26E-07	9.09E-05	5.772082329
ANXA3	1.230549087	11.59874066	6.500596702	9.65E-07	9.23E-05	5.732701088
EMILIN2	1.070315566	8.199351148	6.499181116	9.68E-07	9.23E-05	5.729369653
RP11-6I2.3	1.728935861	7.83577692	6.491871672	9.85E-07	9.36E-05	5.71216383
MTRR	1.016453476	5.064315578	6.465808775	1.05E-06	9.83E-05	5.650762277
CHI3L1	-1.311494132	9.088324889	-6.465397878	1.05E-06	9.83E-05	5.649793602
ANKRD22	2.058144733	8.615873168	6.454062509	1.08E-06	0.00010035	5.623062999
ZAK	1.06538609	7.181386347	6.387277728	1.27E-06	0.000115146	5.465268534
BMX	1.351154601	8.406755918	6.371596279	1.32E-06	0.000117554	5.428142536
FLVCR1	-1.028950698	5.060523707	-6.340894952	1.42E-06	0.000123556	5.355375268
TP53INP2	-1.247576045	8.604134259	-6.325299988	1.48E-06	0.000125887	5.318371536
GRAMD1C	-1.105875646	5.723608674	-6.309701047	1.53E-06	0.000129242	5.281330889
KISS1R	-1.396315458	8.382824392	-6.283883839	1.63E-06	0.000134484	5.219966344
F5	1.284286451	9.716898674	6.279413697	1.65E-06	0.000134484	5.209333775
C19orf60	-1.180430465	10.4375029	-6.279320378	1.65E-06	0.000134484	5.209111784
GPR114	-1.169627434	6.228813575	-6.254235657	1.76E-06	0.000139474	5.149404531
ECHDC3	1.843985927	8.683360609	6.251405849	1.77E-06	0.000139474	5.142664594
TGM3	-1.826926823	7.436237207	-6.250808077	1.77E-06	0.000139474	5.141240727
PIWIL4	1.869455851	7.084017714	6.228944888	1.87E-06	0.000145553	5.089136697
BRI3BP	-1.01325038	6.260437994	-6.216112293	1.93E-06	0.000148597	5.058529939
ZDHHC19	2.093641646	7.742834528	6.199552765	2.01E-06	0.000153769	5.019007755
LHX4-AS1	1.624543601	7.82032171	6.184027501	2.09E-06	0.000157398	4.98192717
LGALS12	-2.030165884	9.044259103	-6.162365804	2.20E-06	0.000163152	4.930147194
LOXL1	1.230336438	6.783268885	6.160118437	2.21E-06	0.000163356	4.924772242
AIM2	1.983964333	9.708431906	6.12927506	2.39E-06	0.000172454	4.850951271

EFEMP2	1.110838042	8.116915323	6.105568259	2.53E-06	0.000178439	4.794143318
HIST1H2AE	1.398575448	8.537724575	6.065181442	2.79E-06	0.000193006	4.697231753
PLP2	1.41059983	9.696493109	6.061482318	2.82E-06	0.00019383	4.688347054
MEF2A	1.21882683	7.17551005	6.056180987	2.86E-06	0.000194561	4.675611693
LOC93622	-1.091139823	7.079885036	-6.03156597	3.04E-06	0.000202295	4.616441981
KLHL2	1.697774885	7.460725554	6.028133814	3.06E-06	0.000203391	4.608186914
BACE2	-1.825987712	6.377760682	-6.024032409	3.09E-06	0.000204834	4.598320618
TOMM40L	1.67117466	10.09341032	6.014178911	3.17E-06	0.000209241	4.574610296
PPM1N	1.011979358	7.49299972	5.958008838	3.64E-06	0.00022966	4.439266607
UBE2F	1.093580524	9.643630266	5.953287122	3.68E-06	0.00022966	4.427875497
C16orf93	-1.146427649	7.571527852	-5.926746074	3.94E-06	0.000240722	4.363805672
CSGALNACT2	1.123005444	5.907496326	5.908884094	4.11E-06	0.000246066	4.320649415
SPNS3	-1.946297472	8.393171653	-5.905982271	4.14E-06	0.000247057	4.3136355
TOPORS	-1.199651036	6.505383878	-5.905045257	4.15E-06	0.000247057	4.311370502
GCH1	2.075280844	8.263894905	5.881404321	4.40E-06	0.000258443	4.254197362
GALNT6	-1.413983108	6.760282547	-5.857865023	4.67E-06	0.000268198	4.197218802
ITIH4	1.100833608	7.312845432	5.812389214	5.23E-06	0.000289578	4.086999303
ZNF274	-1.037132535	9.378614299	-5.808382982	5.28E-06	0.000290993	4.077280581
FAM174A	-1.139654505	6.657216621	-5.803601354	5.34E-06	0.000292249	4.065678977
PFKFB3	1.245679729	11.98113828	5.788065908	5.56E-06	0.000299764	4.027971692
LOC441081	1.382844059	8.025764019	5.775527897	5.73E-06	0.000304961	3.997524408
SPINT1	-1.167104135	7.687308512	-5.767444516	5.85E-06	0.000308143	3.97788755
SLC26A11	2.239407087	7.726082599	5.757289747	6.00E-06	0.00031376	3.953210762
DPEP3	-1.061999344	11.78444076	-5.747511699	6.15E-06	0.000319056	3.929441142
VWA5A	1.35482249	5.46431388	5.731198339	6.40E-06	0.000327754	3.889766772
RTN1	-1.138893611	5.66202417	-5.710716014	6.74E-06	0.000341733	3.83992198
EVL	-1.24434574	8.491266582	-5.699845304	6.92E-06	0.000346281	3.813453502
SGSH	1.109333944	7.505057031	5.694055924	7.03E-06	0.000348115	3.799353331
CLU	1.553201993	7.350488785	5.665931131	7.54E-06	0.000371795	3.730816251

FOLR3	1.035829319	11.47910462	5.647919697	7.88E-06	0.000383703	3.686891264
ZNF211	-1.240630219	7.617223203	-5.63626108	8.12E-06	0.000393309	3.658445522
DDAH2	1.252458142	9.788914776	5.615936169	8.54E-06	0.000405698	3.608829864
RSPH9	1.646046819	8.047138222	5.601735926	8.85E-06	0.000415848	3.574146603
FAIM3	-1.205723865	8.281670366	-5.592552031	9.06E-06	0.000423703	3.551707397
TP53I3	1.824708486	9.011167253	5.57244898	9.53E-06	0.000439525	3.502567324
IL5RA	-1.187920837	6.457765512	-5.569144388	9.61E-06	0.000439525	3.494486706
ACER3	1.258536979	6.602938458	5.522909738	1.08E-05	0.000478485	3.381348171
ZBTB42	-1.139593743	6.390568785	-5.516872472	1.10E-05	0.000483104	3.366563533
LOC100507006	-1.152671486	10.50229777	-5.492637141	1.16E-05	0.000505416	3.307188476
PNP	1.153432368	5.669717965	5.48937766	1.17E-05	0.00050783	3.299199902
JPX	-1.093480342	5.607526444	-5.48753158	1.18E-05	0.00050783	3.29467508
PAQR7	-1.306004465	7.298812503	-5.484502813	1.19E-05	0.000510256	3.287250941
SRGAP2C	-1.018428167	9.099048757	-5.465031868	1.25E-05	0.000530059	3.239509039
ZSCAN18	-1.075014712	6.373737922	-5.443055052	1.32E-05	0.000551092	3.185593067
FBXO34	1.043333677	9.042678648	5.422081002	1.39E-05	0.000571509	3.134108432
PSTPIP2	1.159495222	9.542421639	5.415923744	1.41E-05	0.00057837	3.11898909
MCCC1	-1.105795861	5.432476677	-5.388179348	1.52E-05	0.00060881	3.050833057
CYB561	-1.033959601	7.539790589	-5.375970665	1.56E-05	0.000620959	3.020826945
DOK2	-1.232142174	9.19801999	-5.370950552	1.58E-05	0.000626583	3.008486128
MYO10	1.178339785	5.565618632	5.347889403	1.68E-05	0.000651083	2.951776772
HPGD	2.104699361	5.860994003	5.314433016	1.83E-05	0.000699779	2.869451552
SLC51A	2.660664413	8.051533356	5.313118468	1.83E-05	0.00070087	2.866215633
SLC47A1	-1.235515602	5.149676815	-5.306092312	1.86E-05	0.000709678	2.848918328
LOC101928893	-1.060655524	5.270087543	-5.277672497	2.00E-05	0.000749435	2.778926757
ZNF329	-1.922226243	7.677020569	-5.261865356	2.09E-05	0.000770725	2.739979519
PIK3R6	-1.395859146	7.537987837	-5.237810752	2.22E-05	0.000802718	2.680687813
CAMK1	-1.051424535	6.658799979	-5.219287846	2.32E-05	0.000834221	2.635012383
NDC80	-1.077050936	7.15880186	-5.207558859	2.39E-05	0.000849653	2.606081869

CD81	-1.511317792	9.603165063	-5.198741111	2.45E-05	0.000863018	2.584328119
CST7	1.338966875	12.50804474	5.197102417	2.46E-05	0.00086399	2.580285014
MT1F	1.338595378	9.702668557	5.183395753	2.54E-05	0.000887935	2.546462388
SLC26A8	1.70222651	8.801768526	5.16060872	2.70E-05	0.000922367	2.490215457
BC045789	1.604687953	5.452536357	5.151985934	2.76E-05	0.000938153	2.46892566
ARMC12	1.24661459	4.72723441	5.150825375	2.76E-05	0.000938153	2.466059996
GPR183	-1.759223101	6.801312894	-5.132162129	2.90E-05	0.000964046	2.41996929
MAP1LC3A	-1.093740917	8.355369771	-5.082088518	3.29E-05	0.001057507	2.296244226
SGK1	-1.395673753	10.96983341	-5.024393387	3.81E-05	0.001179192	2.15358528
SDC2	-1.207009181	6.46237724	-5.018301345	3.87E-05	0.001192508	2.138516219
LINC00672	1.016115872	9.502773821	4.987153994	4.19E-05	0.001270061	2.061456097
NQO2	1.083533563	10.41395315	4.985065617	4.21E-05	0.001273054	2.056288486
LIPT1	-1.035819578	5.214528286	-4.963793698	4.45E-05	0.001321202	2.003646238
TMEM119	1.423484542	7.97212649	4.943998665	4.68E-05	0.00137633	1.954650165
PMAIP1	-1.517308885	7.691259491	-4.933680364	4.80E-05	0.00140181	1.929107557
PDGFC	1.232829354	4.572118861	4.918958196	4.99E-05	0.001443495	1.892659987
C5orf30	1.126603278	6.910125507	4.917265252	5.01E-05	0.001447004	1.888468538
CFD	-1.956554063	10.66385055	-4.916958479	5.01E-05	0.001447004	1.887709014
HBD	3.274106476	9.053062495	4.884223027	5.45E-05	0.001528555	1.806652605
AOC3	-1.263664333	7.159220566	-4.87356712	5.60E-05	0.001552444	1.780264271
FCGR1A	1.176945844	10.57721878	4.866041179	5.71E-05	0.001568168	1.761626178
ST6GALNAC3	1.04163649	5.008631302	4.833379865	6.20E-05	0.001666372	1.680733349
SPTSSA	1.266792052	5.019428901	4.831111922	6.24E-05	0.001669828	1.675115959
HLA-DRA	-2.11830424	7.684697418	-4.830557984	6.25E-05	0.001670125	1.673743921
P2RY2	-1.615018733	7.039552682	-4.815328734	6.49E-05	0.001723544	1.636022152
NUP50-AS1	-1.288552472	9.710421608	-4.799031184	6.77E-05	0.001781467	1.595652895
LINC00877	-1.548724274	8.823252234	-4.79076795	6.91E-05	0.001810265	1.575184357
DSC2	1.23042076	8.106242696	4.774335132	7.21E-05	0.00186343	1.534478776
RP11-334C17.5	1.957320536	9.45673276	4.764820654	7.39E-05	0.001897926	1.510910426

C11orf96	1.41893891	6.42994133	4.759980797	7.48E-05	0.001910196	1.498921601
ALOX15	-1.404111747	6.991797446	-4.71415946	8.41E-05	0.00206016	1.385420329
SLC2A1	1.002094326	5.879970448	4.71162586	8.46E-05	0.002066235	1.379144783
HLA-DPA1	-1.35108949	7.263835873	-4.697257296	8.78E-05	0.00211722	1.343555728
FAM20A	1.48413549	4.963360269	4.694394447	8.84E-05	0.002130387	1.336465018
ARFIP1	-1.254293844	8.433977161	-4.689627176	8.95E-05	0.002144562	1.324657593
PRSS33	-2.722694476	11.70526342	-4.666758202	9.49E-05	0.002221275	1.268019596
CAPG	1.055752639	9.481783618	4.663623142	9.57E-05	0.00222779	1.260255667
MCTP1	1.121572816	6.899682498	4.658920723	9.68E-05	0.002249876	1.24861043
HLA-DPB1	-1.28511476	7.266352196	-4.633344968	0.00010337	0.002348029	1.185279082
SLC16A14	-1.169246181	4.831411823	-4.633224064	0.000103402	0.002348029	1.184979722
ZNF266	-1.234895271	8.956354708	-4.605277537	0.000111055	0.00248955	1.115790037
RAB13	1.562075181	8.014987844	4.584606471	0.000117079	0.002568736	1.064622605
MIAT	1.631144653	8.944995295	4.578433786	0.00011894	0.00259642	1.049345056
EBLN2	1.172363915	7.746163893	4.560152599	0.000124628	0.002693431	1.004103957
MLK7-AS1	1.099464531	5.09078696	4.557468756	0.000125486	0.00270387	0.997462854
ERCC1	-1.538162385	8.316919918	-4.524003908	0.000136688	0.002904782	0.914671389
BTN3A1	-1.006822938	9.617281299	-4.521995314	0.000137391	0.002914009	0.909703188
FLVCR1-AS1	-1.513876479	8.170009333	-4.520039689	0.000138079	0.002918577	0.904866126
HLA-DMB	-1.705614497	10.05440596	-4.508859331	0.000142081	0.002966977	0.877214812
HPSE	1.278520403	8.472580944	4.49788377	0.000146121	0.003019328	0.850073928
TRIM22	1.175861373	8.114354815	4.494535581	0.000147377	0.003036575	0.841795171
RPH3A	2.248691208	6.088125986	4.475787692	0.000154607	0.003152565	0.795446237
FBXO6	1.25680741	9.135033917	4.442741	0.000168226	0.003354791	0.713779544
GAFA1	1.215593951	4.518427858	4.440779559	0.000169071	0.003362016	0.708933699
LOC101060510	1.06679116	9.594804368	4.436109184	0.0001711	0.003386814	0.697395938
ITGA7	1.412096014	5.9027015	4.431626237	0.000173071	0.00341708	0.686322068
RP11-499E18.1	1.377474316	5.215093696	4.430360634	0.000173631	0.003421273	0.683195904
RP11-426C22.5	-1.039489337	8.31254147	-4.407914404	0.000183876	0.003555204	0.627763245

LOC100505564	-1.384649826	6.421985167	-4.378063505	0.00019844	0.003741436	0.554080573
CKS2	-1.422255208	7.200648476	-4.360807408	0.000207377	0.003871344	0.51150666
MS4A4A	1.080010257	4.812928299	4.35195933	0.000212115	0.003916948	0.489682927
OR52K3P	-1.048932559	9.408156634	-4.351854052	0.000212172	0.003916948	0.489423285
CD52	-1.507658906	10.08510013	-4.340835012	0.000218224	0.00400139	0.462250907
LCN2	1.843292931	11.16884097	4.316872537	0.000231986	0.004196866	0.403184417
CYSLTR2	-1.384067406	5.162432953	-4.299411346	0.000242555	0.004348112	0.360164719
FBP1	-1.000170714	8.274851832	-4.258067272	0.000269529	0.004710771	0.25838098
MAP4K1	-1.203078396	8.043383747	-4.255500447	0.000271299	0.004737879	0.252065535
SPAG1	-1.028546184	6.01089795	-4.243687903	0.000279593	0.004839425	0.223007699
SLC25A38	-1.144666144	6.254829183	-4.233934077	0.000286632	0.00493796	0.19902155
ALAS2	1.147026674	5.408848378	4.220513302	0.000296606	0.005070425	0.166029063
CXCL8	-1.790656979	9.926020014	-4.220128522	0.000296897	0.005070425	0.165083347
RP11-36B6.1	1.729248276	6.631389381	4.201372591	0.00031143	0.005227915	0.118998404
RARRES3	-1.282646309	10.54835238	-4.196750511	0.000315118	0.005261285	0.107645689
MAOA	2.428365368	5.810126962	4.184754185	0.000324896	0.005380399	0.078188223
ACSF2	-1.011182568	8.006849841	-4.160192883	0.000345863	0.005631328	0.017913125
TPST1	1.184101806	9.188023417	4.127787915	0.000375594	0.005967344	-0.061533054
PTGS2	-1.184635844	6.0010037	-4.094392152	0.000408887	0.006370102	-0.14331031
MMP8	1.200728858	4.711628842	4.087695864	0.000415906	0.006446994	-0.159695209
POMZP3	-1.329635738	6.964538124	-4.080401953	0.000423688	0.006544201	-0.17753752
GDPD5	-1.483309264	7.301160063	-4.053161006	0.000454049	0.006871017	-0.24412794
CLEC1B	1.462527267	8.257723161	4.05122114	0.000456291	0.006880908	-0.2488671
RGL4	1.10344716	9.041920826	4.040507334	0.000468875	0.007031548	-0.275034355
LAMP3	-1.172022241	5.391794655	-3.999224176	0.000520657	0.007592476	-0.375750432
CD69	-1.40815683	5.378339609	-3.996866195	0.00052378	0.007612383	-0.381497464
ACRC	1.065677302	7.914979429	3.994612998	0.000526781	0.007625297	-0.38698853
GSAP	1.025572813	6.085051458	3.975344252	0.000553152	0.007901384	-0.433923285
DMTN	1.215397656	7.698727477	3.968818876	0.000562375	0.007991963	-0.449808143

DPY19L3	1.165107052	7.396269769	3.957261514	0.000579084	0.008169424	-0.477930275
IL18RAP	1.812051354	9.076649389	3.954198247	0.000583595	0.008206324	-0.485381377
AHSP	3.292171868	7.098034615	3.94058322	0.000604065	0.008416923	-0.518485034
BTN3A2	-1.30170241	8.787640302	-3.921359489	0.000634182	0.008725036	-0.565187285
ANKRD55	1.643664906	8.330241602	3.89973876	0.000669827	0.009071356	-0.617657587
MXRA7	1.010139038	6.410520106	3.892823579	0.000681639	0.009166754	-0.634427076
TRBC1	-1.861846559	8.450135054	-3.878235946	0.000707236	0.009453826	-0.669781968
ZNF600	-1.392663714	6.321688268	-3.876962402	0.000709515	0.009472598	-0.672867223
SELENBP1	1.594465189	7.665715412	3.872463536	0.000717625	0.009504686	-0.683764326
NTSR1	1.039489998	6.291613008	3.871051082	0.000720189	0.009532787	-0.687184996
LOC100506922	-1.471170934	7.738120356	-3.859332478	0.00074182	0.009753561	-0.71555466
PPFIBP2	-1.017365769	7.742378803	-3.857095412	0.000746022	0.009790968	-0.720968272
TRMT6	1.047580271	6.196495354	3.844052617	0.000770988	0.01001545	-0.752517619
AKR1C3	1.323293274	5.793567137	3.795782205	0.000870756	0.010924809	-0.869069984
EPB42	2.261607512	6.342388918	3.795287079	0.000871842	0.010932107	-0.870263747
RASGRP1	-1.209546208	6.933565767	-3.738638138	0.001005372	0.01210191	-1.006599354
ASGR2	1.174006049	8.107733198	3.719460956	0.001054978	0.012559406	-1.052638285
LOC101929002	-1.206346389	5.89989934	-3.71496513	0.001066951	0.012640162	-1.06342283
SLC4A1	1.163874045	5.976672342	3.658033875	0.001230603	0.013974147	-1.199695324
LOC100506047	-1.068736411	7.270379937	-3.652606464	0.001247432	0.01409872	-1.212657365
ITGB3BP	1.229293514	6.893481764	3.582170772	0.001487394	0.016080635	-1.380390645
HBM	1.117417969	7.19559696	3.575205614	0.001513443	0.016300413	-1.396926744
AP3B2	1.142434788	5.419938116	3.56333597	0.001558867	0.016637394	-1.425085025
IFIT3	-1.310691531	11.06038052	-3.562175082	0.001563381	0.016669134	-1.427837517
OLFM4	1.696751552	6.771425314	3.513214446	0.001765812	0.018182914	-1.543679508
NGFRAP1	1.24650325	6.994994705	3.501059747	0.001819904	0.018575096	-1.572362039
COQ3	1.064221806	6.449447483	3.443587159	0.002098341	0.02050522	-1.707559757
MADCAM1	-1.102301356	6.960196706	-3.442563249	0.002103659	0.020547923	-1.709961865
GJB6	1.188508559	8.562202394	3.417624396	0.002237335	0.021485359	-1.768396199

CCNA1	1.161441372	4.84647178	3.404045473	0.002313557	0.022022015	-1.800153645
SEMG1	-1.397481226	7.840475793	-3.384630808	0.002426939	0.022840224	-1.84548518
IFIT2	-1.064038573	10.13739285	-3.383703588	0.002432487	0.022882492	-1.84764795
LSM7	-1.480447514	10.07027932	-3.36743167	0.002531877	0.023513276	-1.885569566
C19orf33	1.394014814	7.674240678	3.366339628	0.002538687	0.023541541	-1.888112304
DTX4	-1.015321052	8.180553016	-3.336907634	0.002729062	0.024872824	-1.956533861
HLA-DMA	-1.090090604	8.316509896	-3.335046317	0.002741556	0.024944703	-1.960853811
KLRB1	-1.504819941	6.870379894	-3.332966509	0.002755583	0.025016398	-1.965679844
GNLY	-1.826884135	8.210322325	-3.273915407	0.003184159	0.027794675	-2.102248633
MAFB	1.323873903	10.31065789	3.264947397	0.003254648	0.028200051	-2.122910615
CLC	-1.018965872	12.95097266	-3.263016236	0.003270024	0.028269296	-2.127357173
CD3D	-1.372322604	8.564181344	-3.233619523	0.003512926	0.029646301	-2.194921407
PTPRCAP	-1.012169837	8.041890443	-3.231142138	0.003534175	0.029779203	-2.200604709
CLEC5A	1.01443976	6.973002493	3.209473993	0.003725392	0.030989382	-2.250241499
LTF	1.569519017	9.608054714	3.206828531	0.003749411	0.031107737	-2.256292791
TNNT1	-1.06966026	7.10313987	-3.206282884	0.003754383	0.031107737	-2.257540674
BTN3A3	-1.332756576	7.11950608	-3.205496471	0.003761561	0.031125951	-2.25933904
DAAM2	1.150456521	6.273455493	3.204829617	0.003767658	0.031164494	-2.260863862
BTNL8	-1.297375153	9.560114545	-3.14429466	0.004362665	0.034466805	-2.398758142
FGF13	1.739393726	7.510869561	3.142485136	0.004381776	0.03457994	-2.402863841
ORM1	1.283947896	10.797807	3.139677882	0.004411583	0.03474899	-2.409231427
C3AR1	1.078753858	11.34100564	3.131197542	0.004502817	0.035263116	-2.428452936
LINC00189	-1.302669684	7.460767408	-3.129941827	0.00451648	0.035282963	-2.431297328
NR4A2	-1.026357479	7.73112175	-3.114075446	0.004692584	0.036331035	-2.467196664
CCL23	-1.649769684	7.401182273	-3.057715835	0.005373022	0.039983777	-2.594096803
RP1-93H18.6	-1.021356556	9.546662222	-3.055602591	0.005400293	0.040062493	-2.598835823
DEFA4	1.560575552	10.56054672	2.972401366	0.006585831	0.046034915	-2.784271559
IFIT1	-1.524558601	8.914272911	-2.961278524	0.006762022	0.04691816	-2.808887966
PPBP	1.653019349	10.46043729	2.948178785	0.006975297	0.047977982	-2.837825471

FLJ12120	-1.05853354	5.942161004	-2.938400029	0.00713867	0.048750521	-2.859388431
HDC	-1.378936955	7.725439547	-2.924718939	0.007373371	0.049726049	-2.889500679
ETV7	-1.236050486	7.753844427	-2.923060609	0.007402314	0.049870076	-2.893146242
CD2	-1.24208624	6.604701873	-2.898650411	0.007841071	0.051644291	-2.946695775
FGFBP2	-1.467401503	6.340752648	-2.838227909	0.009035946	0.056997789	-3.07832272
DQ592442	-1.087127031	6.451895974	-2.829631584	0.009219369	0.057710171	-3.096939841
CRISP3	1.386476819	8.219015934	2.81141175	0.009619862	0.059451517	-3.136306561
RNASE6	-1.094632476	9.546624158	-2.785794455	0.010210897	0.06170237	-3.191442209
TUBB2A	1.38247584	6.635831438	2.740703408	0.011335449	0.066432786	-3.287868987
CD24	1.036440135	8.525270484	2.705335655	0.012298187	0.070337955	-3.362933448
ALOX12	1.050934917	5.380955028	2.629260131	0.014635571	0.079461912	-3.52263768
TGFBI	-1.027140271	8.129899538	-2.585212879	0.016172871	0.085420372	-3.613968784
GZMB	-1.90247326	7.826150783	-2.533129396	0.018184797	0.092056326	-3.720845644
CEACAM6	1.153722569	6.634867108	2.517779421	0.018820774	0.093973682	-3.752107661
VSIG4	1.194810444	5.672745236	2.479085142	0.020516746	0.099344536	-3.8304242
SERPING1	-1.33748584	8.712587028	-2.420436214	0.023358771	0.108408527	-3.947762176
MPO	1.103564889	7.080447497	2.381754573	0.025427419	0.114535497	-4.024225359
PF4	1.257779316	9.542825036	2.353238344	0.027058853	0.119337627	-4.080110614
GZMA	-1.144321337	6.246992356	-2.32993047	0.028463005	0.122904562	-4.125478328
HERC5	-1.002460615	7.794289314	-2.262705484	0.032894233	0.135913873	-4.25472834
FAM3B	-1.69053221	7.801418053	-2.11070991	0.045305966	0.168284854	-4.537789986

Supplementary Table 2. The predicted results from DIANA and TargetScan databases

miRNA	PositionintheUTR	seedmatch	context++score	context++scorepercentile	weightedcontext++score	conservedbranchlength	Pct
Conservedsites							
mmu-miR-203-3p.1	423-429	7mer-m8	-0.02	64	-0.02	6.114	0.31
mmu-miR-203-3p.2	423-429	7mer-1A	-0.02	50	-0.02	6.114	0.23
mmu-miR-539-3p	504-510	7mer-1A	-0.11	90	-0.11	4.238	N/A
mmu-miR-381-3p	504-510	7mer-1A	-0.07	85	-0.07	4.238	N/A
mmu-miR-1928	1045-1052	8mer	-0.36	96	-0.07	6.686	0.68
mmu-miR-222-3p	1045-1052	8mer	-0.36	96	-0.07	6.686	0.68
mmu-miR-221-3p	1045-1052	8mer	-0.36	96	-0.07	6.686	0.68
mmu-miR-22-3p	1050-1056	7mer-1A	-0.17	81	-0.03	7.973	0.54
mmu-miR-455-3p.2	1062-1068	7mer-1A	-0.11	79	-0.02	6.174	0.38
mmu-miR-682	1062-1068	7mer-1A	-0.09	76	-0.02	6.174	0.38
mmu-miR-199a-5p	1077-1083	7mer-1A	-0.28	93	-0.05	7.354	0.79
mmu-miR-199b-5p	1077-1083	7mer-1A	-0.28	93	-0.05	7.354	0.79
mmu-miR-145b	1078-1084	7mer-1A	-0.16	89	-0.03	7.18	0.95
mmu-miR-145a-5p	1078-1084	7mer-1A	-0.16	89	-0.03	7.18	0.95
mmu-miR-320-3p	1108-1114	7mer-1A	-0.06	73	-0.01	4.665	N/A
Poorlyconservedsites							
mmu-miR-6361	17-24	8mer	-0.19	83	-0.19	0.716	<0.1
mmu-miR-6369	17-24	8mer	-0.19	83	-0.19	0.716	<0.1
mmu-miR-6410	17-24	8mer	-0.19	82	-0.19	0.716	<0.1
mmu-miR-6413	17-24	8mer	-0.18	80	-0.18	0.716	<0.1
mmu-miR-24-3p	17-24	8mer	-0.18	80	-0.18	0.716	<0.1
mmu-miR-5124b	17-24	8mer	-0.18	80	-0.18	0.716	<0.1
mmu-miR-3106-5p	18-24	7mer-1A	-0.06	68	-0.06	0	N/A
mmu-miR-149-5p	19-25	7mer-m8	-0.14	82	-0.14	0.591	N/A
mmu-miR-7087-3p	20-26	7mer-m8	-0.09	55	-0.09	0	N/A

mmu-miR-7679-5p	21-27	7mer-m8	-0.2	83	-0.2	0	N/A
mmu-miR-7648-3p	22-28	7mer-m8	-0.09	53	-0.09	0	N/A
mmu-miR-6940-5p	22-28	7mer-m8	-0.09	52	-0.09	0	N/A
mmu-miR-762	22-28	7mer-m8	-0.04	48	-0.04	0	N/A
mmu-miR-7048-5p	23-29	7mer-m8	-0.06	35	-0.06	0	N/A
mmu-miR-185-3p	23-29	7mer-m8	-0.04	25	-0.04	0	N/A
mmu-miR-7083-5p	24-30	7mer-m8	-0.16	57	-0.16	0.113	N/A
mmu-miR-673-3p	25-31	7mer-m8	-0.27	81	-0.27	0	N/A
mmu-miR-7648-3p	27-38	non-canonical	N/A	N/A	N/A	0	N/A
mmu-miR-7648-3p	27-38	non-canonical	N/A	N/A	N/A	0	N/A
mmu-miR-5621-3p	30-36	7mer-1A	-0.14	68	-0.14	0	N/A
mmu-miR-296-5p	30-36	7mer-1A	-0.1	57	-0.1	0	N/A
mmu-miR-6379	34-40	7mer-1A	-0.07	56	-0.07	0	N/A
mmu-miR-455-3p.1	38-44	7mer-1A	-0.09	73	-0.09	1.304	0.21
mmu-miR-7214-3p	38-44	7mer-m8	-0.09	66	-0.09	0	N/A
mmu-miR-201-5p	40-46	7mer-m8	-0.04	60	-0.04	0.113	N/A
mmu-miR-7687-3p	41-47	7mer-m8	-0.1	77	-0.1	0.41	N/A
mmu-miR-188-3p	45-51	7mer-1A	-0.16	76	-0.16	0.468	N/A
mmu-miR-1933-3p	56-62	7mer-1A	-0.03	45	-0.03	0	N/A
mmu-miR-6949-5p	63-69	7mer-m8	-0.09	67	-0.09	0	N/A
mmu-miR-7088-5p	64-70	7mer-m8	-0.02	65	-0.02	0	N/A
mmu-miR-3105-5p	67-73	7mer-m8	-0.13	75	-0.13	0	N/A
mmu-miR-3057-5p	70-77	8mer	-0.38	97	-0.38	0	N/A
mmu-miR-5130	70-76	7mer-1A	-0.25	93	-0.25	0	N/A
mmu-miR-6938-5p	70-76	7mer-1A	-0.18	81	-0.18	0	N/A
mmu-miR-9-5p	73-79	7mer-1A	-0.11	78	-0.11	0.375	<0.1
mmu-miR-193a-5p	76-83	8mer	-0.42	97	-0.42	0.338	<0.1
mmu-miR-3091-5p	78-84	7mer-m8	-0.29	93	-0.29	0	N/A
mmu-miR-3961	87-93	7mer-1A	-0.17	73	-0.17	0	N/A

mmu-miR-18a-3p	88-94	7mer-m8	-0.06	61	-0.06	0.113	N/A
mmu-miR-7069-3p	88-94	7mer-m8	-0.05	58	-0.05	0.113	N/A
mmu-miR-7016-3p	90-96	7mer-1A	-0.07	64	-0.07	0.409	N/A
mmu-miR-7239-5p	93-99	7mer-m8	-0.02	40	-0.02	0	N/A
mmu-miR-3101-5p	96-102	7mer-m8	-0.02	32	-0.02	0	N/A
mmu-miR-7087-3p	108-120	non-canonical	N/A	N/A	N/A	0	N/A
mmu-miR-7087-3p	108-120	non-canonical	N/A	N/A	N/A	0	N/A
mmu-miR-3473c	109-115	7mer-1A	-0.1	70	-0.1	0	N/A
mmu-miR-7649-3p	109-115	7mer-1A	-0.05	50	-0.05	0	N/A
mmu-miR-6975-3p	109-115	7mer-1A	-0.01	29	-0.01	0	N/A
mmu-miR-7063-3p	111-117	7mer-m8	-0.04	33	-0.04	0	N/A
mmu-miR-6973b-3p	111-117	7mer-m8	-0.04	33	-0.04	0	N/A
mmu-miR-760-3p	113-119	7mer-1A	-0.07	48	-0.07	0.113	N/A
mmu-miR-7239-3p	113-119	7mer-1A	-0.05	39	-0.05	0.113	N/A
mmu-miR-1291	113-119	7mer-m8	-0.02	30	-0.02	0	N/A
mmu-miR-7029-3p	114-120	7mer-m8	-0.14	80	-0.14	0.113	N/A
mmu-miR-546	116-123	8mer	-0.43	97	-0.43	0	N/A
mmu-miR-6934-5p	117-123	7mer-1A	-0.1	66	-0.1	0	N/A
mmu-miR-6952-5p	117-123	7mer-1A	-0.05	46	-0.05	0	N/A
mmu-miR-6400	119-130	non-canonical	N/A	N/A	N/A	0	N/A
mmu-miR-6400	119-130	non-canonical	N/A	N/A	N/A	0	N/A
mmu-miR-7680-3p	121-127	7mer-m8	-0.04	55	-0.04	0	N/A
mmu-miR-7663-5p	121-127	7mer-m8	-0.02	53	-0.02	0	N/A
mmu-miR-210-5p	128-134	7mer-m8	-0.09	61	-0.09	0.468	N/A
mmu-miR-6919-5p	130-136	7mer-m8	-0.25	92	-0.25	0.409	N/A
mmu-miR-1668	132-138	7mer-m8	-0.1	81	-0.1	0	N/A
mmu-miR-3544-5p	133-140	8mer	-0.18	89	-0.18	0	N/A
mmu-miR-488-3p	134-140	7mer-m8	-0.04	65	-0.04	0.253	N/A
mmu-miR-7681-3p	134-140	7mer-1A	-0.04	58	-0.04	0	N/A

mmu-miR-471-3p	134-140	7mer-1A	-0.01	29	-0.01	0.113	N/A
mmu-miR-1934-3p	138-144	7mer-1A	-0.11	75	-0.11	0	N/A
mmu-miR-7b-5p	149-155	7mer-1A	-0.03	60	-0.03	0.269	<0.1
mmu-miR-7a-5p	149-155	7mer-1A	-0.03	59	-0.03	0.269	<0.1
mmu-miR-6917-5p	150-157	8mer	-0.31	95	-0.31	0	N/A
mmu-miR-5121	154-160	7mer-m8	-0.2	80	-0.2	0	N/A
mmu-miR-7002-5p	157-163	7mer-1A	-0.06	65	-0.06	0	N/A
mmu-miR-326-5p	164-170	7mer-1A	-0.21	82	-0.21	0	N/A
mmu-miR-486b-3p	164-170	7mer-1A	-0.21	71	-0.21	0	N/A
mmu-miR-486a-3p	164-170	7mer-1A	-0.21	71	-0.21	0	N/A
mmu-miR-6954-5p	164-170	7mer-1A	-0.19	67	-0.19	0	N/A
mmu-miR-31-3p	183-189	7mer-m8	-0.16	81	-0.16	0	N/A
mmu-miR-6996-5p	192-203	non-canonical	N/A	N/A	N/A	0	N/A
mmu-miR-6996-5p	192-203	non-canonical	N/A	N/A	N/A	0	N/A
mmu-miR-485-3p	200-206	7mer-m8	-0.02	24	-0.02	0	N/A
mmu-miR-6909-5p	209-215	7mer-m8	-0.31	87	-0.31	0	N/A
mmu-miR-6418-5p	211-217	7mer-1A	-0.13	70	-0.13	0	N/A
mmu-miR-7670-3p	217-223	7mer-1A	-0.01	25	-0.01	0.375	<0.1
mmu-miR-204-5p	217-223	7mer-1A	-0.01	24	-0.01	0.375	<0.1
mmu-miR-211-5p	217-223	7mer-1A	-0.01	24	-0.01	0.375	<0.1
mmu-miR-7002-5p	234-240	7mer-m8	-0.05	62	-0.05	0	N/A
mmu-miR-7091-3p	235-241	7mer-m8	-0.02	21	-0.02	0	N/A
mmu-miR-6973a-5p	238-244	7mer-m8	-0.18	71	-0.18	0	N/A
mmu-miR-3085-5p	244-250	7mer-m8	-0.1	46	-0.1	0	N/A
mmu-miR-423-3p	248-255	8mer	-0.5	94	-0.5	0.299	N/A
mmu-miR-7686-3p	249-255	7mer-m8	-0.26	72	-0.26	0	N/A
mmu-miR-2861	254-260	7mer-m8	-0.16	81	-0.16	0	N/A
mmu-miR-3091-3p	254-260	7mer-m8	-0.19	74	-0.19	0	N/A
mmu-miR-330-3p.2	255-266	non-canonical	N/A	N/A	N/A	0	N/A

mmu-miR-330-3p.2	255-266	non-canonical	N/A	N/A	N/A	0	N/A
mmu-miR-6996-5p	259-266	8mer	-0.21	89	-0.21	0	N/A
mmu-miR-6355	264-270	7mer-m8	-0.03	70	-0.03	0	N/A
mmu-miR-6920-5p	265-271	7mer-m8	-0.02	36	-0.02	0	N/A
mmu-miR-693-5p	268-275	8mer	-0.3	96	-0.3	0	N/A
mmu-miR-3472	271-277	7mer-m8	-0.14	83	-0.14	0	N/A
mmu-miR-295-5p	275-282	8mer	-0.05	84	-0.05	0.113	N/A
mmu-miR-292b-5p	276-282	7mer-1A	-0.05	80	-0.05	0.411	N/A
mmu-miR-294-5p	276-282	7mer-1A	-0.04	75	-0.04	0.411	N/A
mmu-miR-290a-5p	276-282	7mer-1A	-0.01	49	-0.01	1.207	N/A
mmu-miR-292a-5p	276-282	7mer-1A	-0.01	48	-0.01	1.207	N/A
mmu-miR-293-5p	276-282	7mer-1A	-0.01	47	-0.01	1.207	N/A
mmu-miR-5133	284-290	7mer-m8	-0.18	93	-0.18	0	N/A
mmu-miR-6950-5p	285-291	7mer-m8	-0.12	72	-0.12	0	N/A
mmu-miR-6379	286-293	8mer	-0.26	94	-0.26	0	N/A
mmu-miR-7671-5p	291-297	7mer-1A	-0.17	80	-0.17	0	N/A
mmu-miR-149-5p	292-298	7mer-m8	-0.15	83	-0.15	0.264	N/A
mmu-miR-7087-3p	293-300	8mer	-0.32	93	-0.32	0	N/A
mmu-miR-3963	307-313	7mer-1A	-0.11	64	-0.11	0	N/A
mmu-miR-223-5p	309-315	7mer-1A	-0.05	53	-0.05	0.113	N/A
mmu-miR-7089-3p	316-323	8mer	-0.37	98	-0.37	0	N/A
mmu-miR-33-3p	325-331	7mer-m8	-0.02	51	-0.02	0.113	N/A
mmu-miR-7119-3p	331-337	7mer-m8	-0.02	39	-0.02	0	N/A
mmu-miR-1668	343-349	7mer-m8	-0.18	90	-0.18	0	N/A
mmu-miR-7062-5p	351-357	7mer-1A	-0.09	66	-0.09	0	N/A
mmu-miR-3475-3p	352-358	7mer-m8	-0.13	80	-0.13	0	N/A
mmu-miR-6972-5p	352-358	7mer-m8	-0.09	80	-0.09	0	N/A
mmu-miR-6950-5p	353-360	8mer	-0.25	92	-0.25	0	N/A
mmu-miR-483-3p.1	357-363	7mer-1A	-0.01	31	-0.01	0.694	N/A

mmu-miR-7055-3p	360-367	8mer	-0.33	96	-0.33	0	N/A
mmu-miR-33-5p	367-373	7mer-1A	-0.07	81	-0.07	2.639	<0.1
mmu-miR-450b-5p	369-375	7mer-1A	-0.11	85	-0.11	0	N/A
mmu-miR-129-5p	370-376	7mer-m8	-0.02	77	-0.02	1.069	<0.1
mmu-miR-129b-5p	371-377	7mer-m8	-0.02	75	-0.02	0	N/A
mmu-miR-7091-3p	375-381	7mer-m8	-0.16	80	-0.16	0	N/A
mmu-miR-7037-5p	377-383	7mer-m8	-0.26	90	-0.26	0	N/A
mmu-miR-298-5p	381-387	7mer-m8	-0.14	87	-0.14	0	N/A
mmu-miR-6969-5p	382-388	7mer-m8	-0.08	72	-0.08	0	N/A
mmu-miR-5621-3p	393-399	7mer-m8	-0.17	74	-0.17	0	N/A
mmu-miR-1946a	396-403	8mer	-0.52	97	-0.52	0	N/A
mmu-miR-7658-3p	403-409	7mer-1A	-0.07	72	-0.07	0	N/A
mmu-miR-1968-3p	403-409	7mer-1A	-0.01	31	-0.01	0	N/A
mmu-miR-1952	404-411	8mer	-0.31	96	-0.31	0	N/A
mmu-miR-6974-3p	405-411	7mer-1A	-0.04	51	-0.04	0	N/A
mmu-miR-7649-3p	406-412	7mer-m8	-0.11	71	-0.11	0	N/A
mmu-miR-3473c	406-412	7mer-m8	-0.07	60	-0.07	0	N/A
mmu-miR-6908-3p	408-414	7mer-m8	-0.15	86	-0.15	0	N/A
mmu-miR-7013-3p	411-417	7mer-1A	-0.1	83	-0.1	0	N/A
mmu-miR-6911-3p	414-420	7mer-m8	-0.19	91	-0.19	0	N/A
mmu-miR-7227-3p	425-431	7mer-1A	-0.11	92	-0.11	0	N/A
mmu-miR-6984-5p	425-431	7mer-1A	-0.11	88	-0.11	0.445	N/A
mmu-miR-875-3p	425-431	7mer-1A	-0.1	88	-0.1	0	N/A
mmu-miR-7079-3p	429-436	8mer	-0.3	94	-0.3	0	N/A
mmu-miR-7235-3p	431-437	7mer-m8	-0.16	88	-0.16	0.113	N/A
mmu-miR-1936	433-439	7mer-m8	-0.28	97	-0.28	0	N/A
mmu-miR-495-3p	437-443	7mer-m8	-0.13	95	-0.13	0	N/A
mmu-miR-1192	437-443	7mer-m8	-0.13	94	-0.13	0	N/A
mmu-miR-8118	440-447	8mer	-0.14	95	-0.14	0	N/A

mmu-let-7c-1-3p	443-449	7mer-m8	-0.15	89	-0.15	0	N/A
mmu-miR-338-5p	453-459	7mer-1A	-0.01	38	-0.01	0.113	N/A
mmu-miR-1197-3p	469-475	7mer-1A	-0.17	87	-0.17	0	N/A
mmu-miR-7011-5p	476-483	8mer	-0.52	99	-0.52	0	N/A
mmu-miR-6982-5p	477-484	8mer	-0.51	99	-0.51	0	N/A
mmu-miR-8100	477-483	7mer-1A	-0.27	94	-0.27	0	N/A
mmu-miR-1843b-5p	478-484	7mer-1A	-0.19	90	-0.19	0	N/A
mmu-miR-3473f	490-496	7mer-1A	-0.13	92	-0.13	0	N/A
mmu-let-7c-2-3p	504-510	7mer-m8	-0.2	97	-0.2	0.505	N/A
mmu-let-7a-1-3p	504-510	7mer-m8	-0.2	97	-0.2	0.505	N/A
mmu-let-7b-3p	504-510	7mer-m8	-0.18	96	-0.18	0.505	N/A
mmu-miR-98-3p	504-510	7mer-m8	-0.16	94	-0.16	0.505	N/A
mmu-let-7f-1-3p	504-510	7mer-m8	-0.16	94	-0.16	0.505	N/A
mmu-miR-669b-3p	505-511	7mer-m8	-0.12	85	-0.12	0	N/A
mmu-miR-467a-3p	505-511	7mer-m8	-0.1	82	-0.1	0	N/A
mmu-miR-669f-3p	505-511	7mer-m8	-0.1	82	-0.1	0	N/A
mmu-miR-338-5p	508-515	8mer	-0.28	98	-0.26	0.505	N/A
mmu-miR-3094-3p	516-522	7mer-m8	-0.08	84	-0.07	0	N/A
mmu-miR-374b-5p	525-531	7mer-1A	-0.1	90	-0.09	0.299	N/A
mmu-miR-6374	527-533	7mer-m8	-0.16	91	-0.15	0	N/A
mmu-miR-717	534-541	8mer	-0.44	98	-0.4	0	N/A
mmu-miR-3097-3p	535-541	7mer-1A	-0.16	82	-0.15	0	N/A
mmu-miR-871-5p	536-542	7mer-m8	-0.12	84	-0.11	0	N/A
mmu-miR-743a-5p	536-542	7mer-m8	-0.11	83	-0.1	0	N/A
mmu-miR-5625-3p	538-545	8mer	-0.27	95	-0.24	0	N/A
mmu-miR-20a-3p	547-554	8mer	-0.31	96	-0.28	0.113	N/A
mmu-miR-1950	548-554	7mer-1A	-0.1	79	-0.09	0	N/A
mmu-miR-6962-3p	550-556	7mer-1A	-0.09	72	-0.09	0	N/A
mmu-miR-331-5p	554-561	8mer	-0.32	96	-0.3	0	N/A

mmu-miR-6973b-5p	554-561	8mer	-0.23	95	-0.21	0	N/A
mmu-miR-7211-3p	583-589	7mer-m8	-0.31	96	-0.29	0	N/A
mmu-miR-8091	583-589	7mer-m8	-0.31	96	-0.29	0	N/A
mmu-miR-7021-5p	585-591	7mer-m8	-0.2	88	-0.19	0	N/A
mmu-miR-380-3p	589-595	7mer-1A	-0.06	62	-0.06	0	N/A
mmu-miR-202-5p	592-599	8mer	-0.31	96	-0.29	0.113	<0.1
mmu-miR-6896-3p	638-645	8mer	-0.24	96	-0.22	0	N/A
mmu-miR-7119-3p	657-663	7mer-m8	-0.02	39	-0.02	0	N/A
mmu-miR-133a-5p	671-677	7mer-m8	-0.17	89	-0.16	0	N/A
mmu-miR-138-5p	673-679	7mer-1A	-0.2	72	-0.18	0	<0.1
mmu-miR-370-3p	675-682	8mer	-0.29	97	-0.27	0.113	N/A
mmu-miR-3074-5p	677-683	7mer-m8	-0.09	89	-0.09	0	N/A
mmu-miR-7674-3p	681-687	7mer-m8	-0.1	78	-0.1	0	N/A
mmu-miR-292b-3p	685-691	7mer-m8	-0.25	92	-0.23	0	N/A
mmu-miR-7023-3p	694-700	7mer-1A	-0.17	85	-0.16	0	N/A
mmu-miR-7018-3p	694-700	7mer-1A	-0.14	79	-0.13	0	N/A
mmu-miR-7047-3p	694-700	7mer-1A	-0.13	78	-0.12	0	N/A
mmu-miR-7068-3p	694-700	7mer-1A	-0.14	78	-0.13	0	N/A
mmu-miR-1193-3p	697-703	7mer-m8	-0.18	85	-0.17	0	N/A
mmu-miR-370-5p	697-703	7mer-m8	-0.17	83	-0.16	0	N/A
mmu-miR-7119-3p	716-722	7mer-m8	-0.02	39	-0.02	0	N/A
mmu-miR-1192	720-726	7mer-1A	-0.06	87	-0.05	0	N/A
mmu-miR-7a-1-3p	720-726	7mer-1A	-0.03	86	-0.02	0	N/A
mmu-miR-495-3p	720-726	7mer-1A	-0.01	60	-0.01	0	N/A
mmu-miR-540-3p	737-744	8mer	-0.44	98	-0.41	0	N/A
mmu-miR-6915-5p	737-744	8mer	-0.44	98	-0.41	0	N/A
mmu-miR-133b-5p	739-745	7mer-m8	-0.19	89	-0.18	0	N/A
mmu-miR-7036b-3p	741-747	7mer-m8	-0.18	91	-0.16	0	N/A
mmu-let-7b-3p	750-756	7mer-m8	-0.11	88	-0.1	0.874	N/A

mmu-let-7c-2-3p	750-756	7mer-m8	-0.11	88	-0.1	0.874	N/A
mmu-let-7a-1-3p	750-756	7mer-m8	-0.11	88	-0.1	0.874	N/A
mmu-miR-98-3p	750-756	7mer-m8	-0.09	83	-0.08	0.874	N/A
mmu-let-7f-1-3p	750-756	7mer-m8	-0.09	83	-0.08	0.874	N/A
mmu-miR-539-3p	750-756	7mer-1A	-0.05	77	-0.05	1.412	N/A
mmu-miR-381-3p	750-756	7mer-1A	-0.03	70	-0.03	1.412	N/A
mmu-miR-467a-3p	751-757	7mer-m8	-0.04	66	-0.04	0	N/A
mmu-miR-669f-3p	751-757	7mer-m8	-0.04	66	-0.04	0	N/A
mmu-miR-669b-3p	751-757	7mer-m8	-0.04	65	-0.04	0	N/A
mmu-miR-16-2-3p	754-760	7mer-m8	-0.19	92	-0.17	0	N/A
mmu-miR-340-5p	767-773	7mer-1A	-0.01	50	-0.01	2.821	N/A
mmu-miR-6414	776-782	7mer-1A	-0.03	64	-0.03	0	N/A
mmu-miR-6970-5p	776-782	7mer-1A	-0.01	44	-0.01	0	N/A
mmu-miR-7210-5p	781-787	7mer-1A	-0.05	83	-0.04	0	N/A
mmu-miR-543-3p	781-787	7mer-1A	-0.01	65	-0.01	2.897	N/A
mmu-miR-669p-3p	782-788	7mer-m8	-0.11	90	-0.1	0	N/A
mmu-miR-6905-3p	784-790	7mer-1A	-0.07	83	-0.07	0	N/A
mmu-miR-295-5p	790-796	7mer-m8	-0.03	74	-0.03	0	N/A
mmu-miR-711	796-802	7mer-1A	-0.23	94	-0.21	0	N/A
mmu-miR-15a-3p	804-810	7mer-m8	-0.16	88	-0.14	0	N/A
mmu-miR-7240-5p	809-815	7mer-m8	-0.13	81	-0.12	0	N/A
mmu-miR-882	809-815	7mer-1A	-0.08	60	-0.07	0.315	N/A
mmu-miR-7216-5p	809-815	7mer-1A	-0.05	60	-0.04	0	N/A
mmu-miR-185-5p	809-815	7mer-1A	-0.07	52	-0.06	0.315	N/A
mmu-miR-3473a	809-815	7mer-1A	-0.05	46	-0.05	0.315	N/A
mmu-miR-7012-5p	816-822	7mer-m8	-0.12	78	-0.11	0	N/A
mmu-miR-8113	816-822	7mer-m8	-0.12	78	-0.11	0	N/A
mmu-miR-8119	816-822	7mer-m8	-0.06	75	-0.05	0	N/A
mmu-miR-7057-5p	816-822	7mer-m8	-0.09	73	-0.09	0	N/A

mmu-miR-7050-5p	817-823	7mer-m8	-0.04	56	-0.04	0	N/A
mmu-miR-665-3p	818-825	8mer	-0.41	98	-0.38	0.24	N/A
mmu-miR-7222-3p	819-825	7mer-1A	-0.14	85	-0.12	0	N/A
mmu-miR-1956	820-826	7mer-m8	-0.33	93	-0.3	0.113	N/A
mmu-miR-7647-3p	821-827	7mer-m8	-0.21	89	-0.19	0	N/A
mmu-miR-455-3p.1	822-828	7mer-m8	-0.12	78	-0.11	0.299	<0.1
mmu-miR-101b-3p.1	825-831	7mer-1A	-0.05	69	-0.04	0.299	<0.1
mmu-miR-101b-3p.2	825-831	7mer-1A	-0.05	69	-0.04	0.299	<0.1
mmu-miR-101a-3p.2	825-831	7mer-1A	-0.05	69	-0.04	0.299	<0.1
mmu-miR-582-5p	825-831	7mer-1A	-0.05	61	-0.04	0.299	N/A
mmu-miR-208a-5p	830-836	7mer-m8	-0.02	60	0	0.445	N/A
mmu-miR-6415	830-836	7mer-m8	-0.02	60	0	0.445	N/A
mmu-miR-208b-5p	830-836	7mer-m8	-0.02	48	0	0.445	N/A
mmu-miR-693-3p	831-837	7mer-m8	-0.04	76	-0.01	0	N/A
mmu-miR-674-3p	833-839	7mer-1A	-0.08	75	-0.02	0	N/A
mmu-miR-351-3p	852-859	8mer	-0.2	92	-0.04	0	N/A
mmu-miR-599	855-861	7mer-m8	-0.17	83	-0.03	0	N/A
mmu-miR-1970	855-861	7mer-1A	-0.12	74	-0.02	0	N/A
mmu-miR-5129-3p	863-869	7mer-m8	-0.19	86	-0.04	0.672	<0.1
mmu-miR-455-5p	863-869	7mer-m8	-0.18	85	-0.03	0.672	<0.1
mmu-miR-7651-5p	873-879	7mer-m8	-0.15	81	-0.03	0.815	N/A
mmu-miR-6976-5p	878-884	7mer-m8	-0.11	77	-0.02	0	N/A
mmu-miR-7665-5p	878-884	7mer-m8	-0.11	77	-0.02	0	N/A
mmu-miR-7218-5p	881-887	7mer-1A	-0.18	86	-0.03	0	N/A
mmu-miR-7067-5p	881-887	7mer-1A	-0.15	77	-0.03	0	N/A
mmu-miR-7092-5p	888-894	7mer-1A	-0.16	89	-0.03	0	N/A
mmu-miR-6540-5p	888-895	8mer	-0.23	77	-0.04	0.982	<0.1
mmu-miR-124-3p.2	888-895	8mer	-0.21	74	-0.04	0.982	<0.1
mmu-miR-124-3p.1	888-894	7mer-1A	-0.07	73	-0.01	0.982	<0.1

mmu-miR-5624-3p	888-895	8mer	-0.18	70	-0.03	0.982	<0.1
mmu-miR-7002-5p	894-900	7mer-1A	-0.02	42	0	0	N/A
mmu-miR-6375	896-902	7mer-m8	-0.17	91	-0.03	0	N/A
mmu-miR-466l-3p	900-906	7mer-1A	-0.01	34	0	0	N/A
mmu-miR-568	902-908	7mer-m8	-0.04	50	-0.01	0.507	N/A
mmu-miR-344h-3p	902-908	7mer-1A	-0.01	44	0	0.113	N/A
mmu-miR-223-5p	904-910	7mer-1A	-0.09	69	-0.02	0.468	N/A
mmu-miR-669n	906-912	7mer-m8	-0.1	84	-0.02	0.409	N/A
mmu-miR-592-5p	906-912	7mer-1A	-0.07	72	-0.01	0.652	N/A
mmu-miR-6377	908-914	7mer-m8	-0.06	81	-0.01	0	N/A
mmu-miR-935	932-938	7mer-m8	-0.02	23	0	0	N/A
mmu-miR-216c-3p	945-951	7mer-m8	-0.05	51	-0.01	0	N/A
mmu-miR-6908-5p	945-951	7mer-1A	-0.01	28	0	0	N/A
mmu-miR-543-5p	947-953	7mer-m8	-0.15	76	-0.03	0	N/A
mmu-miR-219a-1-3p	948-954	7mer-m8	-0.15	81	-0.03	0	N/A
mmu-miR-7072-5p	952-958	7mer-m8	-0.06	65	-0.01	0.499	N/A
mmu-miR-7030-5p	956-962	7mer-m8	-0.14	61	-0.03	0	N/A
mmu-miR-7075-5p	956-962	7mer-m8	-0.11	52	-0.02	0	N/A
mmu-miR-7076-5p	956-962	7mer-m8	-0.12	52	-0.02	0	N/A
mmu-miR-6971-5p	957-964	8mer	-0.23	72	-0.04	0	N/A
mmu-miR-7024-5p	958-964	7mer-m8	-0.14	66	-0.03	0	N/A
mmu-miR-7119-5p	958-964	7mer-m8	-0.11	60	-0.02	0	N/A
mmu-miR-7023-5p	958-964	7mer-m8	-0.11	57	-0.02	0	N/A
mmu-miR-7073-5p	958-964	7mer-1A	-0.11	48	-0.02	0	N/A
mmu-miR-6941-5p	958-964	7mer-m8	-0.07	45	-0.01	0	N/A
mmu-miR-7212-5p	959-965	7mer-m8	-0.16	80	-0.03	0	N/A
mmu-miR-7117-5p	959-965	7mer-m8	-0.16	79	-0.03	0	N/A
mmu-miR-3083-5p	961-968	8mer	-0.16	73	-0.03	0.409	N/A
mmu-miR-7679-5p	962-968	7mer-1A	-0.13	73	-0.02	0	N/A

mmu-miR-664-5p	962-968	7mer-m8	-0.09	67	-0.02	0.409	N/A
mmu-miR-3473e	962-968	7mer-1A	-0.04	49	-0.01	0.409	N/A
mmu-miR-3473b	962-968	7mer-1A	-0.04	49	-0.01	0.409	N/A
mmu-miR-3085-3p	963-969	7mer-m8	-0.14	78	-0.03	0.763	0.18
mmu-miR-3064-5p	963-969	7mer-m8	-0.14	78	-0.03	0.763	0.18
mmu-miR-871-3p	965-971	7mer-m8	-0.2	83	-0.04	0.113	N/A
mmu-miR-6976-5p	972-978	7mer-m8	-0.07	69	-0.01	0	N/A
mmu-miR-7665-5p	972-978	7mer-m8	-0.07	66	-0.01	0	N/A
mmu-miR-7054-5p	976-982	7mer-m8	-0.13	84	-0.03	0.409	N/A
mmu-miR-6999-5p	976-982	7mer-m8	-0.08	73	-0.02	0.409	N/A
mmu-miR-6244	984-990	7mer-1A	-0.24	85	-0.04	0	N/A
mmu-miR-5120	985-991	7mer-m8	-0.21	88	-0.04	0	N/A
mmu-miR-5710	987-993	7mer-1A	-0.09	65	-0.02	0	N/A
mmu-miR-7229-3p	997-1003	7mer-m8	-0.08	76	-0.01	0	N/A
mmu-miR-672-3p	998-1005	8mer	-0.23	97	-0.04	0.113	N/A
mmu-miR-377-3p	999-1005	7mer-m8	-0.07	51	-0.01	1.069	N/A
mmu-miR-374b-3p	1007-1013	7mer-1A	-0.01	18	0	0	N/A
mmu-miR-544-5p	1010-1016	7mer-1A	-0.05	56	-0.01	0	N/A
mmu-miR-6964-3p	1011-1017	7mer-m8	-0.04	69	-0.01	0	N/A
mmu-miR-1903	1013-1019	7mer-1A	-0.01	31	0	0	N/A
mmu-miR-1191a	1016-1022	7mer-1A	-0.18	91	-0.03	0	N/A
mmu-miR-6516-5p	1062-1069	8mer	-0.22	93	-0.04	0.609	N/A
mmu-miR-450b-5p	1063-1070	8mer	-0.15	90	-0.03	0	N/A
mmu-miR-7078-3p	1067-1073	7mer-1A	-0.01	39	0	0	N/A
mmu-miR-804	1073-1079	7mer-m8	-0.2	89	-0.04	0	N/A
mmu-miR-7680-5p	1078-1085	8mer	-0.22	94	-0.04	0	N/A
mmu-miR-6344	1081-1087	7mer-1A	-0.03	82	-0.01	0	N/A
mmu-miR-7116-3p	1082-1089	8mer	-0.03	89	-0.01	0	N/A
mmu-miR-6951-3p	1082-1089	8mer	-0.03	88	-0.01	0	N/A

mmu-miR-195a-3p	1088-1094	7mer-m8	-0.07	82	-0.01	0	N/A
mmu-miR-338-5p	1089-1096	8mer	-0.18	96	-0.03	0	N/A
mmu-miR-3095-5p	1105-1111	7mer-m8	-0.16	91	-0.03	0	N/A
mmu-miR-9-3p	1108-1114	7mer-m8	-0.12	84	-0.02	1.296	N/A
mmu-miR-204-5p	1133-1139	7mer-m8	-0.07	70	-0.01	0.804	<0.1
mmu-miR-7670-3p	1133-1139	7mer-m8	-0.06	67	-0.01	0.804	<0.1
mmu-miR-211-5p	1133-1139	7mer-m8	-0.06	66	-0.01	0.804	<0.1
mmu-miR-343	1134-1141	8mer	-0.24	95	-0.04	0	N/A
mmu-miR-6976-3p	1135-1141	7mer-m8	-0.17	83	-0.03	0	N/A
mmu-miR-702-3p	1149-1156	8mer	-0.21	82	-0.04	0	N/A
mmu-miR-6393	1150-1156	7mer-m8	-0.1	77	-0.02	0	N/A
mmu-miR-6990-3p	1154-1160	7mer-m8	-0.14	77	-0.03	0	N/A
mmu-miR-7035-3p	1158-1164	7mer-m8	-0.07	67	-0.01	0	N/A
mmu-miR-6367	1160-1166	7mer-m8	-0.08	60	-0.02	0	<0.1
mmu-miR-351-5p	1160-1166	7mer-m8	-0.07	56	-0.01	0	<0.1
mmu-miR-6394	1160-1166	7mer-m8	-0.07	56	-0.01	0	<0.1
mmu-miR-125a-5p	1160-1166	7mer-m8	-0.06	53	-0.01	0	<0.1
mmu-miR-125b-5p	1160-1166	7mer-m8	-0.06	53	-0.01	0	<0.1
mmu-miR-874-3p	1162-1169	8mer	-0.23	91	-0.04	0	N/A
mmu-miR-1231-3p	1162-1168	7mer-1A	-0.17	87	-0.03	0	N/A
mmu-miR-6990-3p	1162-1168	7mer-1A	-0.07	64	-0.01	0	N/A
mmu-miR-6354	1162-1168	7mer-1A	-0.08	57	-0.02	0	N/A
mmu-miR-7660-5p	1163-1169	7mer-m8	-0.06	44	-0.01	0	N/A
mmu-miR-7067-3p	1166-1172	7mer-1A	-0.03	21	-0.01	0	N/A
mmu-miR-7b-5p	1180-1186	7mer-1A	-0.01	35	0	0.205	<0.1
mmu-miR-7a-5p	1180-1186	7mer-1A	-0.01	35	0	0.205	<0.1
mmu-miR-8099	1190-1196	7mer-1A	-0.16	87	-0.03	0	N/A
mmu-miR-1898	1192-1198	7mer-m8	-0.16	72	-0.03	0	N/A
mmu-miR-3964	1196-1202	7mer-1A	-0.11	68	-0.02	0	N/A

mmu-miR-7013-3p	1206-1212	7mer-m8	-0.02	51	0	0	N/A
mmu-miR-770-5p	1210-1216	7mer-m8	-0.23	90	-0.04	0.113	N/A
mmu-miR-29a-3p	1211-1217	7mer-m8	-0.11	66	-0.02	0.113	<0.1
mmu-miR-29c-3p	1211-1217	7mer-m8	-0.11	66	-0.02	0.113	<0.1
mmu-miR-29b-3p	1211-1217	7mer-m8	-0.1	63	-0.02	0.113	<0.1
mmu-miR-6346	1231-1238	8mer	-0.25	95	-0.05	0	N/A
mmu-miR-6350	1231-1238	8mer	-0.21	93	-0.04	0	N/A
mmu-miR-3060-3p	1234-1240	7mer-m8	-0.12	66	-0.02	0	N/A
mmu-miR-7042-5p	1239-1245	7mer-m8	-0.15	85	-0.03	0	N/A
mmu-miR-654-5p	1244-1250	7mer-1A	-0.07	63	-0.01	0	N/A
mmu-miR-7049-3p	1254-1261	8mer	-0.28	92	-0.05	0	N/A
mmu-miR-7044-3p	1255-1261	7mer-m8	-0.1	72	-0.02	0	N/A
mmu-miR-6954-3p	1255-1261	7mer-1A	-0.09	56	-0.02	0	N/A
mmu-miR-7666-3p	1256-1262	7mer-m8	-0.02	61	0	0	N/A
mmu-miR-7086-5p	1264-1270	7mer-m8	-0.08	70	-0.01	0	N/A
mmu-miR-7661-5p	1268-1274	7mer-m8	-0.02	44	0	0	N/A
mmu-miR-3547-3p	1282-1288	7mer-1A	-0.05	51	-0.01	0.113	N/A
mmu-miR-6927-3p	1284-1290	7mer-1A	-0.04	54	-0.01	0	N/A
mmu-miR-7035-3p	1284-1290	7mer-1A	-0.01	30	0	0	N/A
mmu-miR-6945-3p	1284-1290	7mer-1A	-0.01	21	0	0	N/A
mmu-miR-301a-5p	1286-1292	7mer-1A	-0.01	46	0	0.113	N/A
mmu-miR-301b-5p	1286-1292	7mer-1A	-0.01	46	0	0.113	N/A
mmu-miR-6952-3p	1286-1292	7mer-1A	-0.01	38	0	0.113	N/A
mmu-miR-1896	1286-1292	7mer-m8	-0.02	33	0	0	N/A
mmu-miR-216b-5p	1288-1294	7mer-m8	-0.02	30	0	0.613	<0.1
mmu-miR-7086-5p	1297-1303	7mer-m8	-0.18	88	-0.03	0	N/A
mmu-miR-3096-5p	1311-1317	7mer-1A	-0.15	76	-0.03	0	N/A
mmu-miR-3090-5p	1323-1330	8mer	-0.15	89	-0.03	0	N/A
mmu-miR-7213-5p	1323-1329	7mer-1A	-0.1	71	-0.02	0	N/A

mmu-miR-7019-5p	1324-1330	7mer-1A	-0.12	69	-0.02	0	N/A
mmu-miR-6907-5p	1324-1330	7mer-1A	-0.1	64	-0.02	0	N/A
mmu-miR-7021-3p	1326-1337	non-canonical	N/A	N/A	N/A	0	N/A
mmu-miR-7021-3p	1326-1337	non-canonical	N/A	N/A	N/A	0	N/A
mmu-miR-107-5p	1327-1333	7mer-1A	-0.02	32	0	0.113	N/A
mmu-miR-103-2-5p	1327-1333	7mer-1A	-0.02	31	0	0.113	N/A
mmu-miR-103-1-5p	1327-1333	7mer-1A	-0.01	30	0	0.113	N/A
mmu-miR-7008-3p	1328-1335	8mer	-0.2	87	-0.04	0	N/A
mmu-miR-218-5p	1329-1335	7mer-m8	-0.07	65	-0.01	0.113	<0.1
mmu-miR-7002-3p	1329-1335	7mer-m8	-0.04	55	-0.01	0.113	<0.1
mmu-miR-7026-3p	1329-1335	7mer-1A	-0.02	23	0	0	N/A
mmu-miR-6965-3p	1330-1337	8mer	-0.21	90	-0.04	0	N/A
mmu-miR-7043-3p	1331-1337	7mer-1A	-0.11	73	-0.02	0.445	N/A
mmu-miR-7015-5p	1331-1337	7mer-1A	-0.13	73	-0.02	0	N/A
mmu-miR-6950-3p	1335-1341	7mer-m8	-0.07	62	-0.01	0	N/A
mmu-miR-7215-3p	1338-1344	7mer-1A	-0.14	81	-0.03	0	N/A
mmu-miR-7030-3p	1339-1345	7mer-m8	-0.03	41	-0.01	0	N/A
mmu-miR-206-5p	1344-1350	7mer-m8	-0.02	33	0	0	N/A
mmu-miR-338-3p	1348-1354	7mer-m8	-0.02	46	0	0	<0.1
mmu-miR-1934-5p	1368-1374	7mer-m8	-0.25	87	-0.05	0	N/A
mmu-miR-6372	1371-1377	7mer-m8	-0.14	76	-0.03	0	N/A
mmu-miR-1912-3p	1374-1380	7mer-m8	-0.02	67	0	0	N/A
mmu-miR-6902-5p	1379-1385	7mer-m8	-0.06	72	-0.01	0	N/A
mmu-miR-6918-3p	1385-1391	7mer-1A	-0.03	30	-0.01	0	N/A
mmu-miR-28a-3p	1391-1397	7mer-m8	-0.02	28	0	0	N/A
mmu-miR-3068-5p	1406-1412	7mer-m8	-0.05	56	-0.01	0	N/A
mmu-miR-6934-5p	1409-1415	7mer-m8	-0.15	77	-0.03	0	N/A
mmu-miR-7672-5p	1409-1415	7mer-1A	-0.07	58	-0.01	0	N/A
mmu-miR-6910-3p	1412-1418	7mer-1A	-0.02	35	0	0	N/A

mmu-miR-6910-5p	1420-1426	7mer-1A	-0.2	76	-0.04	0	N/A
mmu-miR-7006-5p	1420-1426	7mer-1A	-0.12	37	-0.02	0	N/A
mmu-miR-5132-5p	1422-1428	7mer-m8	-0.26	84	-0.05	0	N/A
mmu-miR-8110	1424-1430	7mer-m8	-0.31	87	-0.06	0	N/A
mmu-miR-28a-3p	1434-1440	7mer-m8	-0.09	76	-0.02	0.569	N/A
mmu-miR-708-3p	1435-1441	7mer-m8	-0.05	52	-0.01	0	N/A
mmu-miR-350-3p	1440-1446	7mer-1A	-0.01	18	0	0	N/A
mmu-miR-677-3p	1447-1453	7mer-m8	-0.02	53	0	0	N/A
mmu-miR-133a-5p	1460-1466	7mer-m8	-0.02	21	0	0	N/A
mmu-miR-138-5p	1462-1468	7mer-1A	-0.11	53	-0.02	0.819	<0.1
mmu-miR-6926-3p	1468-1474	7mer-1A	-0.01	35	0	0	N/A
mmu-miR-1193-3p	1471-1477	7mer-m8	-0.11	76	-0.02	0.605	N/A
mmu-miR-370-5p	1471-1477	7mer-m8	-0.12	76	-0.02	0.605	N/A
mmu-miR-6904-3p	1479-1485	7mer-m8	-0.12	76	-0.02	0	N/A
mmu-miR-5619-5p	1488-1494	7mer-1A	-0.19	86	-0.04	0	N/A
mmu-miR-668-3p	1488-1494	7mer-1A	-0.05	64	-0.01	0.72	N/A
mmu-miR-7215-5p	1499-1505	7mer-m8	-0.02	53	0	0	N/A
mmu-miR-344h-3p	1508-1514	7mer-m8	-0.02	74	0	0	N/A
mmu-miR-6910-3p	1513-1519	7mer-1A	-0.11	79	-0.02	0	N/A
mmu-miR-1264-5p	1535-1541	7mer-1A	-0.04	38	-0.01	0	N/A
mmu-miR-1934-5p	1536-1542	7mer-m8	-0.16	75	-0.03	0	N/A
mmu-miR-763	1539-1545	7mer-m8	-0.02	51	0	0	N/A
mmu-miR-1955-5p	1543-1549	7mer-m8	-0.04	33	-0.01	0	N/A
mmu-miR-6350	1548-1554	7mer-m8	-0.02	35	0	0	N/A
mmu-miR-6346	1548-1554	7mer-m8	-0.02	29	0	0	N/A
mmu-miR-761	1549-1555	7mer-m8	-0.02	55	0	0.113	N/A
mmu-miR-214-3p	1549-1555	7mer-m8	-0.02	41	0	0.113	N/A
mmu-miR-383-3p	1551-1557	7mer-m8	-0.02	24	0	0.113	N/A
mmu-miR-9769-5p	1553-1560	8mer	-0.06	47	-0.01	0	N/A

mmu-miR-871-3p	1557-1563	7mer-m8	-0.08	62	-0.02	0	N/A
mmu-miR-7222-3p	1561-1567	7mer-m8	-0.19	90	-0.04	0	N/A
mmu-miR-3090-3p	1563-1569	7mer-1A	-0.03	56	-0.01	0	N/A
mmu-miR-3096-5p	1573-1579	7mer-m8	-0.07	55	-0.01	0	N/A
mmu-miR-486a-3p	1584-1590	7mer-1A	-0.11	48	-0.02	0	N/A
mmu-miR-486b-3p	1584-1590	7mer-1A	-0.11	48	-0.02	0	N/A
mmu-miR-6954-5p	1584-1590	7mer-1A	-0.09	44	-0.02	0	N/A
mmu-miR-326-5p	1584-1590	7mer-1A	-0.05	42	-0.01	0	N/A
mmu-miR-5120	1585-1591	7mer-m8	-0.23	90	-0.04	0	N/A
mmu-miR-5710	1587-1593	7mer-1A	-0.05	47	-0.01	0	N/A
mmu-miR-692	1590-1596	7mer-1A	-0.04	68	-0.01	0	N/A
mmu-miR-6896-3p	1591-1597	7mer-1A	-0.01	39	0	0	N/A
mmu-miR-6240	1598-1604	7mer-m8	-0.04	54	-0.01	0.253	N/A
mmu-miR-330-3p.1	1598-1604	7mer-m8	-0.02	38	0	0.253	N/A
mmu-miR-218-5p	1610-1616	7mer-m8	-0.02	35	0	1.818	<0.1
mmu-miR-7002-3p	1610-1616	7mer-m8	-0.02	34	0	1.818	<0.1
mmu-miR-7008-3p	1610-1616	7mer-1A	-0.01	21	0	0	N/A
mmu-miR-7026-3p	1610-1616	7mer-1A	-0.01	14	0	0	N/A
mmu-miR-6965-3p	1611-1617	7mer-m8	-0.02	37	0	0.729	N/A
mmu-miR-339-5p	1614-1620	7mer-1A	-0.01	27	0	0.113	N/A
mmu-miR-7665-3p	1614-1625	non-canonical	N/A	N/A	N/A	0	N/A
mmu-miR-7665-3p	1614-1625	non-canonical	N/A	N/A	N/A	0	N/A
mmu-miR-8118	1623-1629	7mer-m8	-0.02	37	0	0	N/A
mmu-miR-1955-5p	1632-1639	8mer	-0.28	92	-0.05	0	N/A
mmu-miR-219b-5p	1635-1641	7mer-m8	-0.19	82	-0.04	0.468	N/A
mmu-miR-1942	1637-1643	7mer-m8	-0.02	50	0	0	N/A
mmu-miR-7229-3p	1640-1646	7mer-m8	-0.02	45	0	0	N/A
mmu-miR-672-3p	1641-1647	7mer-m8	-0.11	88	-0.02	0.113	N/A
mmu-miR-669c-3p	1642-1649	8mer	-0.08	56	-0.02	0	N/A

mmu-miR-466i-3p	1643-1650	8mer	-0.18	89	-0.03	0	N/A
mmu-miR-362-3p	1643-1649	7mer-1A	-0.04	76	-0.01	0.113	N/A
mmu-miR-329-3p	1643-1649	7mer-1A	-0.03	69	-0.01	0.113	N/A
mmu-miR-654-3p	1657-1663	7mer-m8	-0.16	86	-0.03	0.707	N/A
mmu-miR-6381	1674-1680	7mer-m8	-0.15	82	-0.03	0	N/A
mmu-miR-6924-5p	1675-1681	7mer-m8	-0.02	16	0	0	N/A
mmu-miR-7011-5p	1676-1682	7mer-m8	-0.05	50	-0.01	0	N/A
mmu-miR-6942-5p	1677-1683	7mer-m8	-0.06	54	-0.01	0	N/A
mmu-miR-6916-5p	1677-1683	7mer-m8	-0.05	47	-0.01	0	N/A
mmu-miR-6952-3p	1684-1690	7mer-m8	-0.04	68	-0.01	0	N/A
mmu-miR-301b-5p	1684-1690	7mer-m8	-0.02	65	0	0	N/A
mmu-miR-301a-5p	1684-1690	7mer-m8	-0.02	65	0	0	N/A
mmu-miR-7084-3p	1685-1691	7mer-m8	-0.02	37	0	0	N/A
mmu-miR-7074-3p	1689-1695	7mer-1A	-0.03	42	-0.01	0	N/A
mmu-miR-6924-5p	1696-1702	7mer-1A	-0.08	48	-0.02	0	N/A
mmu-miR-1967	1696-1702	7mer-1A	-0.01	23	0	0	N/A
mmu-miR-6985-5p	1698-1704	7mer-m8	-0.24	93	-0.04	0	N/A
mmu-miR-1936	1703-1709	7mer-m8	-0.15	89	-0.03	0	N/A
mmu-miR-493-5p	1711-1717	7mer-m8	-0.06	76	-0.01	0	N/A
mmu-let-7g-3p	1712-1718	7mer-m8	-0.2	82	-0.04	0	N/A
mmu-miR-7224-3p	1716-1722	7mer-1A	-0.14	83	-0.03	0	N/A
mmu-miR-6974-3p	1717-1723	7mer-m8	-0.11	76	-0.02	0	N/A
mmu-miR-7671-5p	1720-1726	7mer-1A	-0.2	85	-0.04	0	N/A
mmu-miR-7029-3p	1721-1728	8mer	-0.33	95	-0.06	0.113	N/A
mmu-miR-7091-3p	1722-1728	7mer-1A	-0.15	78	-0.03	0	N/A
mmu-miR-6902-3p	1725-1731	7mer-1A	-0.07	62	-0.01	0	N/A
mmu-miR-1933-5p	1727-1733	7mer-1A	-0.14	69	-0.03	0	N/A
mmu-miR-182-5p	1734-1740	7mer-m8	-0.1	64	-0.02	1.653	0.14
mmu-miR-664-5p	1759-1765	7mer-1A	-0.11	72	-0.02	0	N/A

mmu-miR-10b-3p	1786-1792	7mer-1A	-0.19	93	-0.04	0	N/A
mmu-miR-7221-3p	1793-1799	7mer-1A	-0.09	56	-0.02	0	N/A
mmu-miR-468-3p	1794-1800	7mer-m8	-0.09	75	-0.02	0	N/A
mmu-miR-7048-3p	1799-1805	7mer-m8	-0.05	70	-0.01	0	N/A
mmu-miR-7077-3p	1799-1805	7mer-m8	-0.05	67	-0.01	0	N/A
mmu-miR-1224-5p	1805-1811	7mer-m8	-0.14	89	-0.03	0.113	N/A
mmu-miR-7026-5p	1808-1814	7mer-1A	-0.05	56	-0.01	0	N/A
mmu-miR-7079-3p	1811-1817	7mer-m8	-0.16	81	-0.03	0	N/A
mmu-miR-208b-3p	1827-1833	7mer-1A	-0.11	77	-0.02	0.264	<0.1
mmu-miR-208a-3p	1827-1833	7mer-1A	-0.1	75	-0.02	0.264	<0.1
mmu-miR-499-5p	1827-1833	7mer-1A	-0.04	50	-0.01	0.264	<0.1
mmu-miR-3066-3p	1830-1836	7mer-1A	-0.01	43	0	0	N/A
mmu-miR-1a-2-5p	1832-1839	8mer	-0.27	96	-0.05	0	<0.1
mmu-miR-1a-1-5p	1832-1839	8mer	-0.27	95	-0.05	0	<0.1
mmu-miR-485-3p	1834-1840	7mer-1A	-0.1	75	-0.02	0	N/A
mmu-miR-205-5p	1836-1842	7mer-m8	-0.19	93	-0.04	0.113	<0.1
mmu-miR-703	1839-1845	7mer-m8	-0.1	87	-0.02	0	N/A
mmu-miR-7062-5p	1854-1860	7mer-m8	-0.37	96	-0.07	0	N/A
mmu-miR-764-3p	1855-1861	7mer-m8	-0.2	93	-0.04	0.113	N/A
mmu-miR-5110	1856-1862	7mer-m8	-0.16	84	-0.03	0	N/A
mmu-miR-7081-5p	1856-1862	7mer-m8	-0.19	81	-0.03	0	N/A
mmu-miR-7086-5p	1857-1863	7mer-m8	-0.18	89	-0.03	0	N/A
mmu-miR-7661-5p	1861-1867	7mer-m8	-0.02	44	0	0	N/A
mmu-miR-539-5p	1863-1869	7mer-1A	-0.01	48	0	0.679	N/A
mmu-miR-706	1863-1869	7mer-1A	-0.01	45	0	0	N/A
mmu-miR-126a-5p	1870-1876	7mer-1A	-0.07	84	-0.01	0.789	N/A
mmu-miR-126b-5p	1872-1878	7mer-1A	-0.01	38	0	0	N/A
mmu-miR-497a-3p	1884-1890	7mer-1A	-0.09	87	-0.02	0	N/A
mmu-miR-489-5p	1889-1895	7mer-1A	-0.17	83	0	0	N/A

Note: miR, microRNA.